JOURNAL OF GEOPHYSICAL RESEARCH, VOL. 92, NO. B9, PAGES 9135–9152, AUGUST 10, 1987

Polar Basal Melting on Mars

STEPHEN M. CLIFFORD

Lunar and Planetary Institute, Houston, Texas

If ice is present throughout the cryosphere anywhere on Mars, thermodynamic considerations suggest that it is most likely at the poles. Given this condition, the deposition of dust and H_2O at the polar surface will ultimately result in a situation where the equilibrium depth to the melting isotherm has been exceeded, melting ice at the base of the cryosphere until thermal equilibrium is once again established. Should deposition persist, the polar deposits will ultimately reach a thickness where melting will occur at their actual base. At this point the cap may reach a state of equilibrium, where the deposition of any additional ice is balanced by geothermal melting. Thermal calculations yield basal melting thicknesses that are consistent with the inferred 4–6 km thickness of the present north polar cap; however, in the south the deposits appear sufficiently thin (1–2 km) that geothermal melting is likely to be relegated to a depth that lies well below the regolith-polar cap interface. Similar conclusions are reached from consideration of the polar caps' theoretical equilibrium profiles. In the north a basal yield stress characteristic of ice at or near the melting point is indicated, while in the south it appears the cap has yet to achieve the necessary height for significant deformation to occur at its base. The potential importance of basal melting is illustrated through the discussion of four examples: (1) the origin of the major polar reentrants, (2) the removal and storage of an ancient Martian ice sheet, (3) the mass balance of the polar terrains, and (4) the possibility of basal melting at temperate latitudes. This analysis suggests that the process of basal melting may play a key role in understanding the evolution of the Martian polar terrains and the long-term climatic behavior of water on Mars.

INTRODUCTION

The Martian cryosphere has been defined as that region of the crust where the temperature remains continuously below the freezing point of water [*Fanale*, 1976; *Rossbacher and Judson*, 1981]. Its extent is determined by the latitudinal variation of mean annual surface temperatures, the thermal conductivity of the regolith, and the value of the Martian geothermal heat flux. On the basis of reasonable estimates of these variables, present thermal models suggest that the depth to the 273 K isotherm varies from about 1–3 km at the equator to approximately 3–8 km at the Martian poles (Figure 1) [*Fanale*, 1976; *Rossbacher and Judson*, 1981; *Crescenti*, 1984].

Recent estimates of the total inventory of H_2O on Mars [*McElroy et al.*, 1977; *Pollack and Black*, 1979; *Carr*, 1986] are sufficiently large ($\gtrsim 10^7$ km^3) that, at least near the poles, ice may be present throughout the cryosphere. If so, then the deposition and retention of any material at the polar surface will result in a situation where the equilibrium depth to the melting isotherm has been exceeded, melting ice at the base of the cryosphere until thermodynamic equilibrium is once again established.

Water that results from basal melting will drain and fill the available pore space that exists beneath the frozen outer crust. Theoretical calculations indicate that the total pore volume of the crust is substantial and may be sufficient to store a quantity of water equivalent to a global layer nearly 1.5 km deep [*Clifford*, 1981*a*, 1984*a*]. Possible consequences of this large storage potential, viewed in the context of basal melting, will be discussed later in this paper.

Polar basal melting has been cited as a potentially important process in the climatic cycling of H_2O on Mars and in the evolution of the Martian polar terrains [*Clifford and Huguenin*, 1980; *Clifford*, 1980*a,b,c*; *Howard*, 1981]. In this paper the thermal requirements and implications of this process will be discussed in greater detail.

Paper number 7B4003.
1048-0227/87/007B-4003$05.00

A GEOLOGIC SUMMARY OF THE MARTIAN POLAR TERRAINS

Composition

While Mariner 7 thermal and spectroscopic observations confirmed that CO_2 is the dominant constituent of the Martian seasonal caps [*Neugebauer et al.*, 1971], the composition of the much smaller remnant caps remained uncertain until the arrival of the Viking mission in 1976. Viking Infrared Thermal Mapper (IRTM) observations of the perennial north polar ice revealed summertime brightness temperatures as high as 205 K, well in excess of the 148 K sublimation temperature of CO_2 [*Kieffer et al.*, 1976]. Concurrent water vapor column abundance measurements made by the Viking Mars Atmospheric Water Detectors (MAWD) confirmed that the atmosphere above the cap was saturated with respect to a surface reservoir of H_2O at 205 K [*Farmer et al.*, 1976]. These observations demonstrated conclusively that the composition of the volatile component of the remnant cap was water ice.

Although the high summer temperatures recorded by Viking eliminated any possibility of a CO_2 ice component in the perennial cap, they also provided strong evidence that the polar deposits consisted of something other than simply water ice alone. IRTM measurements indicated that the polar ice had an albedo of 0.45, a figure far below the value of 0.7 that characterizes clean terrestrial snow. *Kieffer et al.* [1976] attributed the low albedo of the ice to the deposition and subsequent entrainment of atmospheric dust, a conclusion reached earlier by *Cutts* [1973*a*] and *Cutts et al.* [1976] based on an analysis of Mariner 9 and Viking high-resolution imagery. These images revealed the existence of numerous horizontal layers of a dark material, presumably dust, interbedded with the polar ice.

With the identification of H_2O in the north, it was expected that the composition of the south perennial cap would also

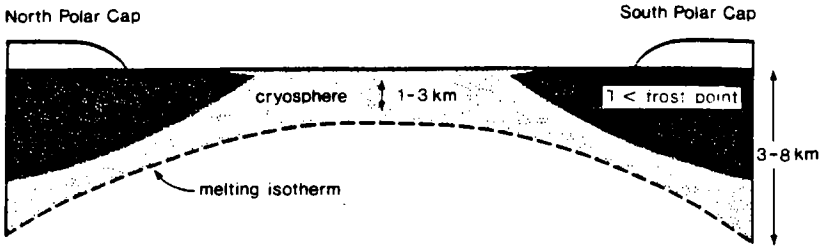

Fig. 1. A pole-to-pole cross section of the Martian crust illustrating the theoretical latitudinal variation in depth of the 273 K isotherm. Ground ice can exist in equilibrium with the atmosphere only at those latitudes and depths where crustal temperatures are below the frost point (~198 K [*Farmer and Doms*, 1979]). Outside these polar reservoirs, ground ice can only survive if it is diffusively isolated from the atmosphere by a regolith of low gaseous permeability [e.g., *Smoluchowski*, 1968; *Clifford and Hillel*, 1983; *Fanale et al.*, 1986]. Figure adapted from *Fanale* [1976] and *Rossbacher and Judson* [1981].

prove to be water ice. Yet, throughout the following southern summer, Viking IRTM observations failed to reveal south polar surface temperatures much in excess of 148 K [*Kieffer*, 1979]. Atmospheric water vapor levels were also considerably lower than those previously recorded in the north [*Davies and Wainio*, 1981; *Jakosky and Farmer*, 1982]. These observations led *Kieffer* [1979] to conclude that the south perennial cap had remained covered with CO_2 throughout the Martian year.

The year-round survival of the southern CO_2 cover has been attributed to a spring albedo that was 33% higher than observed for the equivalent season in the north [*Paige and Ingersoll*, 1985]. *Paige and Kieffer* [1986] suggest that this hemispheric asymmetry is the result of the greater insolation received during southern spring. They argue that the rapid heating of dust grains entrained in the seasonal CO_2 deposit causes them to sink into the frost, resulting in a dramatic increase in the deposit's surficial reflectivity.

Whatever the reason for the survival of the CO_2 cover, *Jakosky and Farmer* [1982] note that for as long as such a condition persists, the south polar cap will act as a cold trap for atmospheric H_2O, indicating that it must be at least partially composed of water ice. Further support for this conclusion comes from the earth-based observations of *Barker et al.* [1970], who reported high hemispheric water vapor column abundance measurements during the southern summer of 1969. This observation appears to indicate that the southern cap occasionally loses its mantle of CO_2, exposing an underlying reservoir of water ice [*Jakosky and Farmer*, 1982].

Geology

The north and south polar terrains represent both the youngest and the most complex surfaces to be found on Mars. The two principal geologic units common to both poles are (1) the remnant ice cap, and (2) the polar layered deposits [*Murray et al.*, 1972; *Soderblom et al.*, 1973*a*,*b*]. In the north these terrains overlie the moderately cratered plains, while in the south they blanket the ancient (~4 b.y. old) heavily cratered highlands [*Murray et al.*, 1972; *Soderblom et al.*, 1973*a*].

The extreme youth of the polar terrains is supported by Viking high-resolution images of the north polar region. These images reveal that within the $\sim 8 \times 10^5$ km^2 covered by the layered deposits, there are no craters with diameters greater than 300 m. As noted by *Cutts et al.* [1976], this observation argues for an age of the exposed surface which is less than 10^6 years.

In the north the layered deposits occupy the region poleward of 80°N. The remnant ice cap, which has a diameter of roughly 1000 km [*Carr*, 1981], overlies and appears to be genetically related to these deposits. Both units are characterized by numerous, laterally extensive, horizontal layers that have individual thicknesses of 14–46 m [*Blasius et al.*, 1982]. Their combined thickness, estimated from Mariner 9 radio occultation data, appears to reach a maximum of 4–6 km near the center of the cap [*Dzurisin and Blasius*, 1975].

Within the remnant cap, individual layers appear to be composed predominantly of water ice, with a small and stratigraphically variable component of entrained dust [*Toon et al.*, 1980]. Beyond the edge of the cap, exposures of the layered deposits appear markedly darker, an observation that suggests a lower ice-to-dust ratio [*Cutts et al.*, 1979]. Alternatively, these differences might also reflect variations in the dust grain size distribution or the extent of frost coverage on local slopes (F. P. Fanale, personal communication, 1984).

As seen in Figure 2, the most distinctive characteristic of the northern cap is the pattern of dark parallel linear troughs that swirl outward in a counterclockwise direction from the pole [*Soderblom et al.*, 1973*a*; *Cutts et al.*, 1976; *Howard et al.*, 1982]. Individual troughs are typically several hundred kilometers long and 5–15 km wide and reach depths of 0.1–1 km; while the surface slopes, exhibited by their bordering scarps, may be as steep as 8° [*Howard et al.*, 1982]. Also visible in Figure 2 are several major erosional reentrants. The largest of these, Chasma Boreale (85°N, 0°W), originates deep within the interior of the cap and extends outward to its edge over a distance of some 500 km.

In the south the small remnant cap (~350 km diameter) is centered at 86°S, 30°W [*Carr*, 1981]. It is superimposed on an extensive region of defrosted layered deposits (approximately 1500 km in diameter) whose areal coverage is roughly twice that occupied by the equivalent unit in the north [*Soderblom et al.*, 1973*a*]. As in the north, the southern deposits appear to be composed of 40 or more individual layers, each layer averaging some 30 m in thickness. Radio occultation data [*Dzurisin and Blasius*, 1975] suggest that these deposits reach a maximum height of 1–2 km in the vicinity of 87°S, 0°W.

Similar to its northern counterpart, the most notable features of the southern cap are the dark troughs that spiral clockwise and outward from the pole. There are also several major erosional reentrants within the defrosted layered deposits. The largest of these, Chasma Australe (88°S, 270°W), has roughly the same general scale, shape, and orientation as Chasma Boreale in the north.

Origin and Evolution

Since Mariner 9 obtained the first clear photographs of the polar terrains in 1971, a general consensus has developed regarding the active constructional and erosional processes

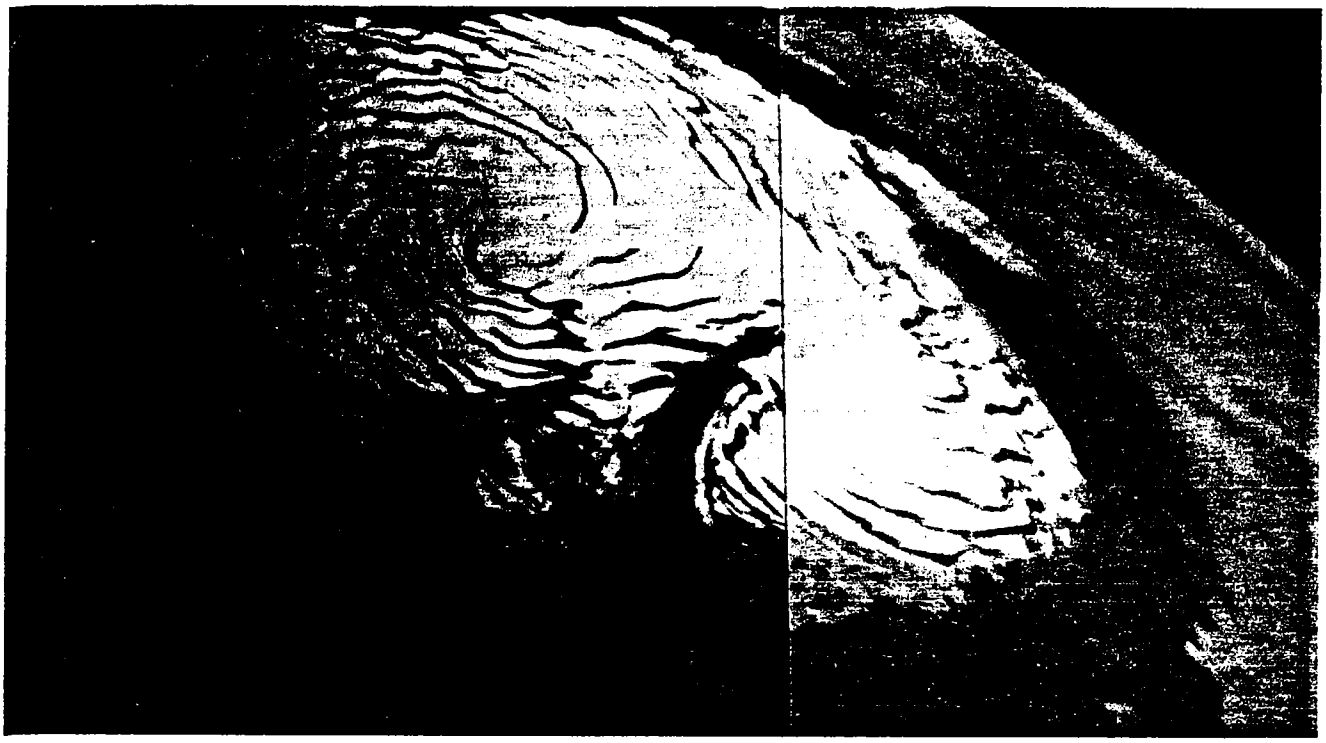

Fig. 2. The Martian north polar cap as seen by Viking (811A01, 811A02). The large channel-like feature near the center of the photograph is Chasma Boreale, while the polar troughs are visible as the dark spiral pattern emanating from the center of the cap.

responsible for their origin [*Howard et al.*, 1982]. An essential element of this model is the belief that atmospheric dust, raised during the Martian global dust storms, acts as nucleation centers for H_2O ice condensation. As either hemisphere enters the fall season, these suspended particles receive an additional coating of frozen CO_2 that makes them heavy enough to precipitate from the atmosphere, thus contributing to the growth of both the seasonal and permanent caps [*Cutts*, 1973*a*; *Pollack et al.*, 1979].

Observational support for this depositional model comes from images returned by Viking Lander 2 (48°N, 225.6°W) during its first 2 years of operation. The images revealed the sudden appearance of a reddish-tinted "snow" in early fall [*Jones et al.*, 1979; *Wall*, 1981; *Guinness et al.*, 1982]. This thin snow cover persisted throughout the northern winter and became patchy by early spring. However, it was not until many weeks after surface temperatures had risen above the CO_2 frost point that all the condensate finally disappeared, leaving behind a thin veneer of dust. This observation appears to confirm the existence of a significant H_2O ice component within the seasonal deposit [*Jones et al.*, 1979; *Wall*, 1981; *Guinness et al.*, 1982].

The ultimate fate of the dust and H_2O that precipitates from the atmosphere during the formation of the seasonal cap is a function of the latitude at which final deposition occurs. At the very highest and coldest latitudes, where H_2O ice is in equilibrium with the water vapor content of the atmosphere, the ice-rich depositional layer persists throughout the year, thus adding to the perennial cap. However, at those latitudes where diurnal temperatures rise significantly above the frost point, any surface H_2O is eventually lost by sublimation. What remains is a thin (microns thick) seasonal mantle of dust that extends from the periphery of the polar caps to the latitudes of ±40°. In some regions there is evidence that local winds episodically remove and redistribute this eolian deposit [*Arvidson et al.*, 1983], while in other regions it may accumulate from year to year, forming a blanket of debris that covers the local terrain [*Soderblom et al.*, 1973*b*].

The banded nature of the polar terrains suggests that the depositional and erosional balance at the poles has been modulated by periodic variations in insolation resulting from cyclical changes in the Martian obliquity and orbital elements [*Murray et al.*, 1973; *Ward*, 1974; *Toon et al.*, 1980; *Cutts and Lewis*, 1982]. For example, the obliquity oscillates about a mean value of 24.4° with a period of 1.2×10^5 years [*Ward*, 1979]. The amplitude of this oscillation also varies and reaches a theoretical maximum of 13.6° every 1.3×10^6 years [*Ward*, 1979]. At low obliquity, both seasonal temperature fluctuations and mean annual polar temperatures are at a minimum. This situation is reversed during times of high obliquity, when summers of continuous illumination alternate with winters of total darkness, producing both extreme seasonal variations and higher mean annual temperatures at the poles. Other variables include the 5.1×10^4 year precessional cycle and two superposed periods of change in orbital eccentricity, a 9.5×10^4 year cycle with a peak-to-peak amplitude of 0.04, and a 2×10^6 year cycle with an amplitude of 0.1 [*Murray et al.*, 1973; *Ward*, 1974, 1979; *Toon et al.*, 1980]. However, while the precessional cycle and variations in orbital eccentricity will affect the peak value and duration of summer polar insolation, only changes in obliquity actually alter the mean annual insolation at a particular latitude.

Assuming radiative equilibrium, mean annual surface temperatures at the poles can be calculated from

$$T_s = \left[\frac{\langle I \rangle_{\text{pole}} (1 - A_b)}{\epsilon \sigma} \right]^{1/4} \quad (1)$$

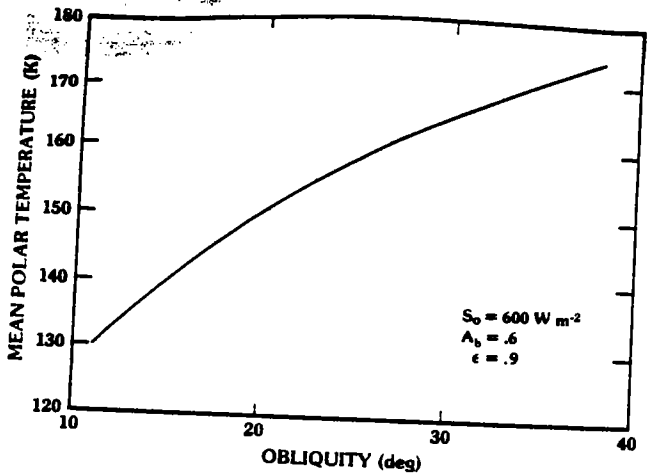

Fig. 3. Mean annual polar surface temperatures as a function of obliquity.

where A_b is the polar cap albedo, ϵ is the emissivity of the polar ice, σ is the Stefan-Boltzmann constant, and $\langle I \rangle_{pole}$ is the mean annual polar insolation. $\langle I \rangle_{pole}$ is given by

$$\langle I \rangle_{pole} = \frac{S_0 \sin i}{\pi(1 - e^2)^{1/2}} \quad (2)$$

where S_0 is the solar constant at 1.52 AU, i is the obliquity, and e is the orbital eccentricity [*Hoffert et al.*, 1981].

In Figure 3, mean polar surface temperatures are plotted as a function of obliquity. Assuming a time-averaged albedo of 0.6 and an emissivity of 0.9, obliquities of 10.8°–38° produce temperatures in the range of 129 K–174 K. Variations in orbital eccentricity will affect these results by only a few tenths of a degree. As a point of reference, the current value of obliquity (25.2°) and orbital eccentricity (0.09) yields a mean polar temperature of 159 K [*Ward*, 1979].

Astronomically driven temperature variations can affect the evolution of the polar terrains in several ways. For example, the cold polar temperatures that characterize low obliquities may result in the equatorward advance of the polar terrains by as much as several degrees. By the same token, the warmer temperatures associated with high obliquities should shift these borders closer to the poles. This suggests that the current polar boundaries are only a surface manifestation of the present insolation balance; therefore, at depth, they may be interbedded over considerable distances [*Squyres*, 1979].

In addition to modulating the areal extent of the polar deposits, climatic variations can also influence the quantity of material that is deposited and retained by the caps. For example, at low obliquity, when the poles are at their coldest, CO_2 ice caps should persist throughout the year. In that event, the atmospheric pressure may fall to the point where dust can no longer be elevated from the planet's surface [*Ward*, 1974; *Fanale and Cannon*, 1979; *Toon et al.*, 1980; *Fanale et al.*, 1982]. This cessation of dust storm activity could drasticly reduce or eliminate H_2O deposition at the poles [*Toon et al.*, 1980; *Fanale et al.*, 1982]. So too, at times of high obliquity, sublimation due to high polar surface temperatures may substantially reduce or eliminate the H_2O component of the annual depositional layer. Therefore significant polar accumulation may occur only under climatic conditions similar to those we observe at present [*Toon et al.*, 1980; *Cutts and Lewis*, 1982].

BASAL MELTING

In terrestrial glacial studies the term "basal melting" is used to describe any situation where the local geothermal heat flux, as well as any frictional heat produced by glacial sliding, is sufficient to raise the temperature at the base of an ice sheet to its melting point. In this regard, the process is always discussed with reference to the interface between an ice sheet and the bed on which it rests. As illustrated in Figure 4, however, it may be appropriate to broaden the use of this term as it applies to Mars.

Figure 4*a* is an idealized cross section of the Martian polar crust as it would have appeared prior to the deposition of any dust or ice. As noted earlier, present thermal models suggest that under such conditions the 273 K isotherm should lie 3–8 km beneath the surface [*Fanale*, 1976; *Rossbacher and Judson*, 1981; *Crescenti*, 1984]. With temperatures that range well below the frost point, the polar crust represents the dominant thermodynamic sink for H_2O on Mars; therefore, if ice is present in the cryosphere anywhere on the planet, it seems most likely at the poles.

Given the above conditions, the deposition of dust and H_2O at the polar surface will result in a situation where the equilibrium depth to the melting isotherm is exceeded (Figure 4*b*). In response to this added layer of insulation the position of the melting isotherm will rise within the crust until thermal equilibrium is once again established. Thus, while melting will not occur at the actual base of the polar deposits, it will occur at the base of the cryosphere in response to any increase in polar deposit thickness. Should deposition continue, the polar deposits will eventually reach the required thickness for "true" basal melting to occur (Figure 4*c*). Since this last stage is merely the endpoint in the evolution of a single continuous process, use of the term "basal melting" is broadened here to include any situation where pore or glacial ice is melted as the result of a rise in the position of the melting isotherm, regardless of whether such melting occurs at the actual base of the deposits or within the underlying terrain.

Thermal Calculations

The polar deposit thickness required for basal melting can be calculated by solving the one-dimensional steady state heat conduction equation. After *Weertman* [1961*a*], this thickness is given by

$$H = k_{eff} \frac{(T_{mp} - T_{ms})}{Q_g + Q_f} \quad (3)$$

where k_{eff} is the effective thermal conductivity of the deposits, T_{mp} is the melting point temperature of the ice, T_{ms} is the mean polar surface temperature, Q_g is the geothermal heat flux, and Q_f is the frictional heat due to glacial sliding.

The thermal conductivity of the polar deposits is determined by such factors as the volumetric mixing ratios of ice and dust, their spatial variability, temperature-dependent thermal properties, and the presence of other contaminants. While a comprehensive analysis of these factors is beyond the scope of this paper, a reasonable range of values can be inferred from the available data. For example, the light-scattering properties of the dust suspended in the Martian atmosphere indicate grain diameters in the range of 0.2–2.5 μm [*Pang et al.*, 1976; *Pollack et al.*, 1979; *Chylek and Grams*, 1978]. If this size range is

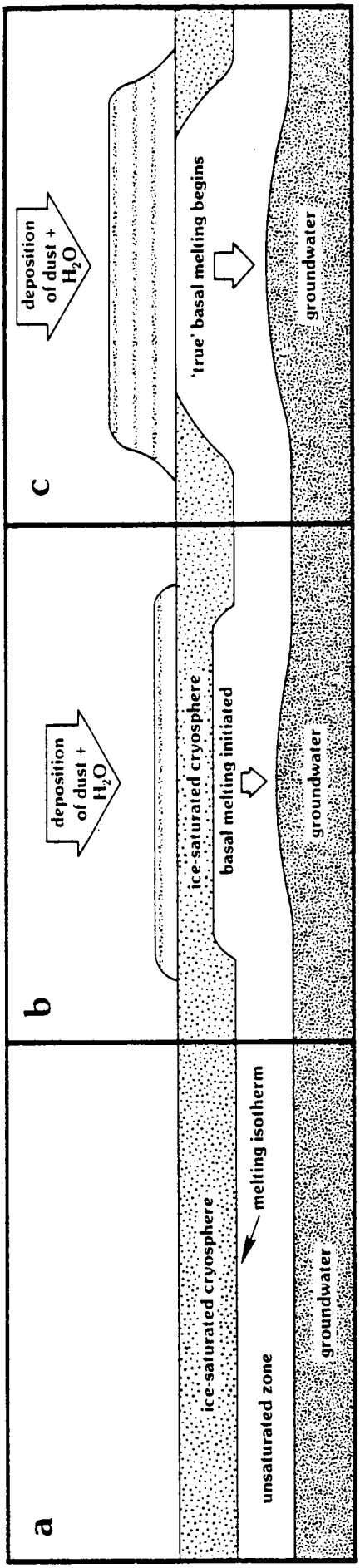

Fig. 4. An idealized cross section of the polar crust illustrating the possible time evolution of basal melting. The sequence depicts (*a*) a time prior to the deposition of any dust and ice, (*b*) the onset of deposition and basal melting, and (*c*) melting at the actual base of the deposits.

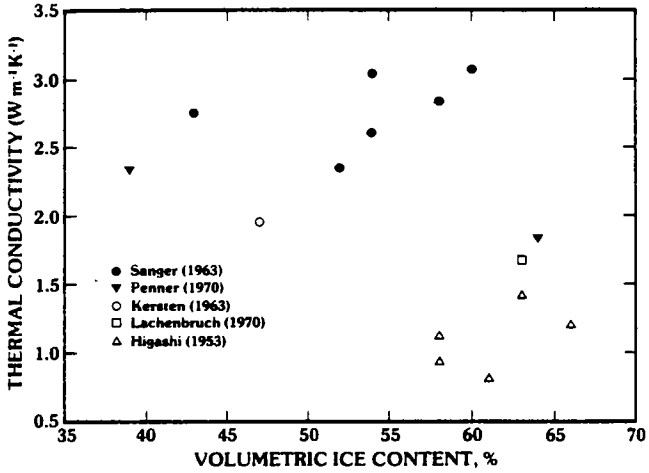

Fig. 5. Thermal conductivities of various terrestrial clay-ice mixtures as a function of their ice content. (Additional information is presented in Table 1.)

representative of the dust entrained in the polar ice, then the thermal properties of the polar deposits should be closely approximated by laboratory mixtures of clay and ice.

The thermal conductivities of various clay-ice mixtures are plotted as a function of their volumetric ice content in Figure 5, while additional information on each mixture is presented in Table 1. Roughly half the mixtures possess conductivities comparable to that of ice (~2.25–3.5 W m^{-1} K^{-1}), while the rest have values that are lower. Since the conductivities of virtually all clay minerals equal or exceed that of ice [*Clark*, 1966; *Horai and Simmons*, 1969], it appears difficult to explain how any mixture of the two components could have a lower value. Indeed, in frozen soils, where the volume fraction of clay-size particles is negligible, the resulting thermal conductivities are uniformly high [*Kersten*, 1963; *Sanger*, 1963; *Jumikis*, 1966; *Penner*, 1970; *Lachenbruch*, 1970; *Lachenbruch et al.*, 1982]. This suggests that the low conductivity exhibited by many clay-ice mixtures may be attributable to physical properties that are unique to the clay-size mineral fraction.

Experimental evidence presented by *Penner* [1970] suggests that the low conductivity of clay-rich soils may be due to the presence of thin films of unfrozen water ($k \sim 0.54$ W m^{-1} K^{-1}) adsorbed on the clay component. Such films can exist down to very low temperatures [*Anderson et al.*, 1967; *Anderson and Tice*, 1973], particularly in the presence of potent freezing point depressors such as NaCl and $CaCl_2$ [*Banin and Anderson*, 1974]. Since the quantity of H_2O adsorbed per unit surface area is roughly constant for all mineral soils [*Puri and Murari*, 1963], it follows that the unfrozen water content of a frozen soil will be proportional to the soil's content of high specific surface area clay. Thus the range of conductivities depicted in Figure 5 may simply reflect differences in the quantity, specific surface area, and geochemical nature of the clay component.

Another important factor that can influence the thickness required for basal melting is the melting temperature of the polar ice. The melting point may be depressed by both pressure and solute effects; however, the effect of pressure, 7.43×10^{-8} K Pa^{-1} [*Hobbs*, 1974], is extremely small. For example, the pressure exerted by a 6-km-thick polar cap ($\rho \sim 10^3$ kg m^{-3}) will lower the basal melting temperature by less than 2 K. The potential effect of salt is far greater. The existence of various salts in the regolith is supported by the discovery of a duricrust layer at both Viking Lander sites and by the elemental

TABLE 1. Physical and Thermal Properties of Terrestrial Clay-Ice Mixtures

Description	T, K	Volumetric Ice Content, %	Thermal Conductivity, W m^{-1} K^{-1}	Reference
Clay soil	263	43	2.75	*Sanger* [1963]
Clay soil	263	52	2.35	*Sanger* [1963]
Clay soil	263	54	3.03	*Sanger* [1963]
Clay soil	263	54	2.61	*Sanger* [1963]
Clay soil	263	58	2.84	*Sanger* [1963]
Clay soil	263	60	3.06	*Sanger* [1963]
Sudbury silty-clay	253	39	2.34	*Penner* [1970]
Leda silty-clay	253	64	1.84	*Penner* [1970]
Fairbanks silty-clay loam	269	47	1.95	*Kersten* [1963]
Clay soil	-	63	1.67	*Lachenbruch* [1970]
Black soil (38% clay and silt)	268	58	1.13	*Higashi* [1953]
Black soil (38% clay and silt)	268	63	1.42	*Higashi* [1953]
Brown soil (27% clay and silt)	268	58	0.94	*Higashi* [1953]
Brown soil (27% clay and silt)	268	66	1.21	*Higashi* [1953]
Yellow-brown soil (47% silt and clay)	268	61	0.82	*Higashi* [1953]

composition of the soil as determined by the inorganic chemical analysis experiments on board each spacecraft [*Toulmin et al.*, 1977; *Clark*, 1978; *Clark and Van Hart*, 1981]. In light of this evidence, it seems likely that salts are also present in the polar dust. Among the most commonly cited candidates are $CaCl_2$ (218 K eutectic), $MgCl_2$ (238 K), and NaCl (252 K) [*Clark*, 1978; *Brass*, 1980]. It should be noted, however, that serious questions have been raised concerning the chemical and thermodynamic stability of $CaCl_2$ and $MgCl_2$ under ambient Martian conditions, particularly in the presence of abundant sulfates [*Clark and Van Hart*, 1981]. Given these arguments, brines based on NaCl appear to be the most likely candidates to be found in the polar ice.

The presence of even a small quantity of salt may be important, for it opens the possibility that melting may occur not at a discrete depth defined by a particular isotherm but over a broad range of temperatures representing an equally broad range of depths within the polar ice [*Ricq-de Bouard*, 1977]. For example, in terrestrial temperate glaciers, water is typically found in microscopic veins, some tens of μm in diameter, along the three-grain intersections of ice crystals and as small lenses along ice-grain boundaries [*Nye and Mae*, 1972; *Raymond and Harrison*, 1975]. *Nye and Frank* [1973] suggest that these veins may form a three-dimensional drainage network that results in the transport of heat (by advection), as well as dissolved gasses and solutes [*Raymond and Harrison*, 1975]. By such a system, water that is produced by the presence of solutes and by heat arising from the deformation of the ice may drain to the base of the cap.

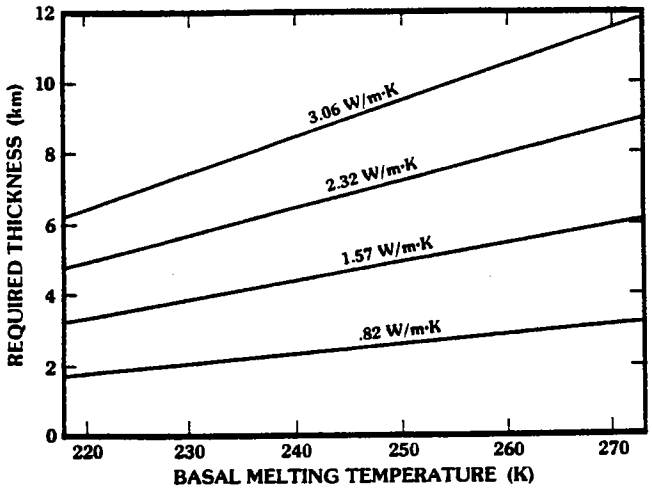

Fig. 6. Polar deposit thicknesses required for basal melting based on a mean annual surface temperature of 157 K, a geothermal heat flux of 3×10^{-2} W m^{-2}, and thermal conductivities covering the range from 0.82 to 3.06 W m^{-1} K^{-1}.

Basal melting thicknesses, calculated from a reasonable range of thermal conductivities and melting temperatures, are summarized in Figure 6 and Table 2. The results, which range from 1.7 to 12 km, are based on a mean polar surface temperature of 157 K (corresponding to a mean obliquity of 24.4°) and a Martian geothermal heat flux of 3×10^{-2} W m^{-2} [*Fanale*, 1976]. Note that this estimate of the geothermal heat flux is the most conservative of the three values that have so far appeared in the literature. The two higher estimates are the 3.5×10^{-2} W m^{-2} figure of *Toksöz and Hsui* [1978] and the value of 4×10^{-2} W m^{-2} cited by *Davies and Arvidson* [1981]. No frictional heat input due to glacial sliding was assumed.

The basal melting thicknesses summarized in Table 2 raise considerable doubt as to whether the Martian polar caps are presently cold-based. Indeed, even if "true" basal melting does not presently occur at the poles, melting at the base of the cryosphere (Figure 4*b*) appears to be an inevitable consequence of polar deposition. If so, a geothermal heat flux of 3×10^{-2} W m^{-2} has the potential for melting as much as 5×10^{-3} m of ice from beneath the polar caps each Martian year.

Of course, should glacial sliding occur, the resulting frictional heat could substantially reduce the required thickness for basal melting and substantially increase the production of meltwater. For a given basal sliding velocity V_b the frictional heat flux Q_f can be calculated from

$$Q_f = V_b \tau_b$$

$$= V_b \rho_i g h \frac{dh}{dx} \quad (4)$$

where τ_b is the basal shear stress, ρ_i is the density of the polar

TABLE 2. Calculated Basal Melting Thicknesses

Polar Deposit Thermal Conductivity, W m^{-1} K^{-1}	Basal Melting Temperatures		
	218 K	252 K	273 K
0.82	1.67	2.60	3.17
1.57	3.19	4.97	6.07
2.32	4.72	7.35	8.97
3.06	6.22	9.69	11.8

Thicknesses are in kilometers.

These results are based on a mean polar surface temperature of 157 K and geothermal heat flux of 3×10^{-2} W m^{-2}.

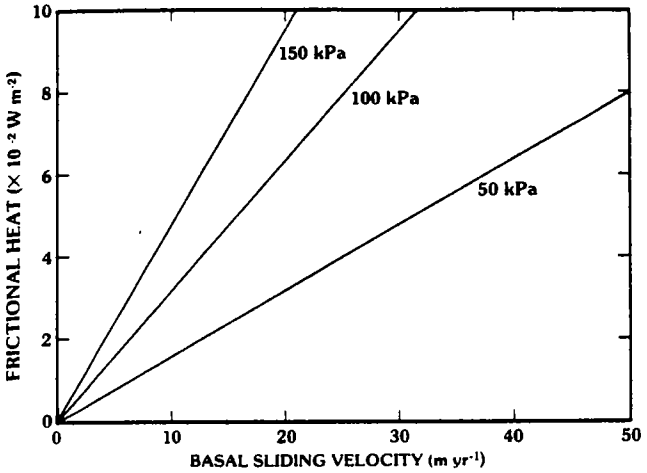

Fig. 7. Frictional heat produced by basal sliding under an applied basal shear stress of 50, 100, and 150 kPa.

ice (including any component of entrained dust), g is the acceleration of gravity (3.73 m s^{-2}), h is the local thickness of the cap, and dh/dx is the local slope of the cap's surface [*Weertman*, 1961*a*]. As seen in Figure 7, a sliding velocity of 10 m yr^{-1}, driven by a basal shear stress of 100 kPa, generates sufficient heat (3×10^{-2} W m^{-2}) to halve the calculated thicknesses for basal melting presented in Table 2.

Finally, climatic variations in polar surface temperature and mass balance can also influence basal melting thicknesses. However, while variations in such factors as the Martian obliquity can produce significant oscillations in mean annual surface temperature, the amplitude of the resulting thermal wave is attenuated rapidly with depth (Figure 8). Thus even at the very shallowest depths at which basal melting is possible, obliquity variations will produce only a 25–100 m change in the position of the melting isotherm.

Changes in polar mass balance have a less obvious but potentially more important effect. For example, if the rate of polar deposition increases faster than the rate at which the deposits can thermally reequilibrate, then the thickness required for basal melting will necessarily increase. Similarly, a high rate of ablation will cause a reduction in this thickness [*Weertman*, 1961*a*]. Thus the combination of long-term changes in surface temperature and mass balance can result in situations where the melting isotherm periodically rises to the base of the polar deposits, while at other times it may lie well below this interface (Figures 4*b* and 4*c*).

Flow Calculations

It has been said that current polar temperatures on Mars are too cold to permit glacial flow [e.g., *Sharp*, 1974: *Howard et al.*, 1982; *Lucchitta*, 1984]. However, both theoretical studies and field observations of terrestrial glaciers indicate that virtually all of the deformation associated with glacial flow occurs near an ice sheet's base, where the temperature and shear stress are greatest [*Nye*, 1959]. This fact and the results of the thermal calculations presented in the previous section suggest that contrary to earlier beliefs, polar glacial flow on Mars cannot be ruled out simply on the basis of low polar surface temperatures.

An observation that may provide some insight as to whether the base of either Martian polar cap is currently at the melting point is a comparison between the caps' observed and theoretical equilibrium profiles [*Orowan*, 1949; *Nye*, 1959; *Weertman*, 1961*b*; *Clifford*, 1984*b*] . Such a comparison is useful because the profile of an ice cap is to a large extent determined by the mechanical properties of its basal ice, properties that are, in turn, sensitively dependent on temperature. To minimize any confusion that might arise in this discussion, all references to polar cap thickness and basal temperature are made with regard to the interface between the polar deposits and the bed on which they rest.

For glacial ice the strain rate is related to the shear stress by Glen's law

$$\dot{\epsilon} = A\,\tau^n \tag{5}$$

where n is a constant with a value of ~3 [*Weertman*, 1973], and A is the flow law constant that is a function of temperature, crystal size, crystal orientation, and impurity content [*Paterson*, 1981]. The temperature dependence of A is given by the Arrhenius equation

$$A = A_0 \exp(-Q/RT) \tag{6}$$

where A_0 has a value of $\sim 4.3 \times 10^{-4}$ s^{-1} kPa^{-3}, Q is the activation energy for creep (139 kJ mol^{-1} for 263 K $\leq$ T $\leq$ 273 K, 60 kJ mol^{-1} for T $\leq$ 263 K), and R is the gas constant [*Weertman*, 1973; *Paterson*, 1981].

In Figure 9, A is plotted for the temperature range that is likely to characterize the Martian polar ice at its surface and at depth. The resulting variation in A covers some 9 orders of magnitude. Because of this strong temperature dependence, even a slight reduction in ice temperature necessitates a large increase in shear stress to produce a given strain rate. This is evident in Figure 10, where the strain rate of ice is plotted as a function of shear stress for both 273 K and 263 K. The implications of this temperature dependence on the equilibrium profile of an ice cap are significant.

A major contribution toward understanding the origin of ice sheet profiles was made by *Orowan* [1949], who argued that the mechanical properties of ice are reasonably approximated

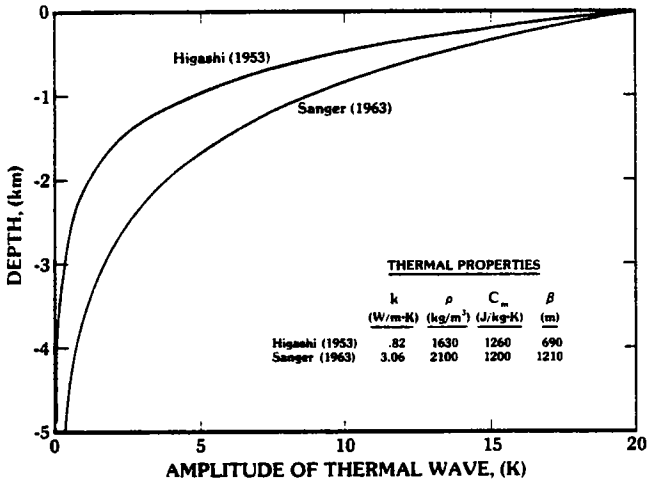

Fig. 8. Maximum amplitude of the obliquity driven temperature variation as a function of depth in two compositional analogs of the Martian polar ice. The 13° oscillation in Martian obliquity produces a corresponding oscillation in surface temperature, $\Delta T(0)$, of ~20 K (equation (1)). The amplitude of this variation as a function of depth is given by $\Delta T(z) = \Delta T(0) \exp(-z/\beta)$, where β is the obliquity skin depth. Note that $\beta = \sqrt{Pk/\pi\rho_i C_m}$, where P is the obliquity period (1.2×10^5 years), k is the polar deposit thermal conductivity, ρ_i is the density, and C_m is the specific heat.

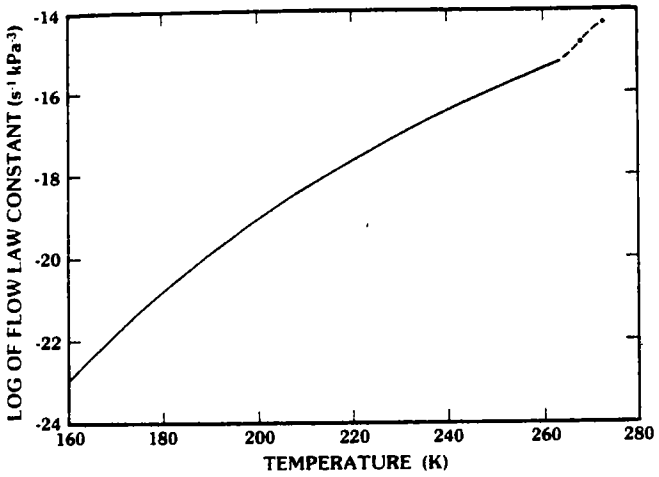

Fig. 9. The temperature dependence of the flow law constant for ice. The deviation in the curve at temperatures above 263 K corresponds to a change in the activation energy of creep (see text).

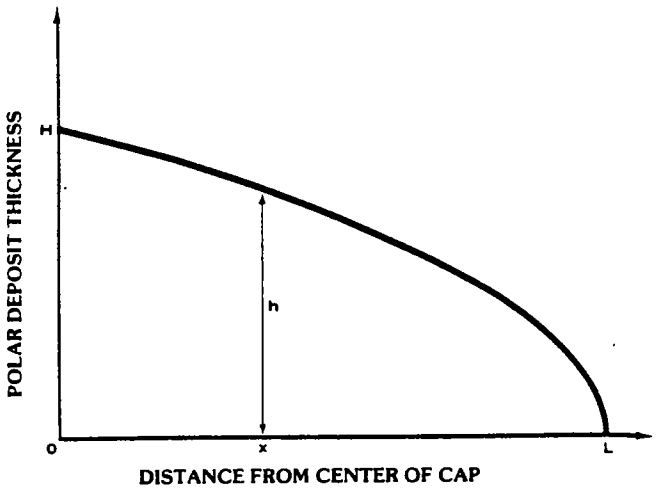

Fig. 11. *Orowan's* [1949] model for the equilibrium profile of an ice sheet.

by the assumption of perfect plasticity (i.e., where the strain rate is considered zero below a certain critical yield stress and infinite for any stress above). This approximation is equivalent to replacing A in equation (5) with $C\tau_0^{-n}$, where C is a constant, τ_0 is the basal yield stress, and the resulting expression is evaluated at the limit $n \rightarrow \infty$ [*Paterson*, 1981]. For ice at 273 K, τ_0 is generally assumed to be 100 kPa [*Orowan*, 1949; *Nye*, 1959; *Weertman*, 1964, 1966; *Paterson*, 1981], corresponding to a strain rate, given by equation (5), of 5.3×10^{-9} s^{-1}. As seen in Figure 10, a shear stress of 217 kPa is required to achieve this same strain rate at 263 K.

Based on the assumption of perfect plasticity, Orowan proposed a simple model for the equilibrium profile of an ice sheet, whereby the mass an ice sheet gains by deposition over its surface is balanced by what it loses through flow and ablation at its perimeter. Orowan's model is illustrated in Figure 11, where an ice sheet of half width L, resting on a horizontal base, is seen in cross section. At a distance x from the ice sheet's center the force (per unit width) driving the outward flow of the ice is equal to the mean hydrostatic pressure ($1/2\ \rho_i\ gh$) times the height over which the pressure is exerted (h). In equilibrium this hydrostatic force is balanced by the shear resistance of the basal ice that lies external to x (i.e., $\tau_b(L - x)$), or more simply

$$\frac{1}{2}\rho_i\, gh^2 = \tau_b(L - x) \tag{7}$$

Solving equation (7) for h, we find that the height of the ice sheet, a distance x from its center, is given by

$$h = \left[\left(\frac{2\tau_b}{\rho_i\, g}\right)(L - x)\right]^{1/2} \tag{8}$$

Orowan's model has been remarkably successful at reproducing the observed profiles of many terrestrial ice sheets and glaciers. For example, the Greenland ice cap, at a latitude of 72°N, has a half width of approximately 450 km and a central height of 3200 m [*Orowan*, 1949; *Nye*, 1951; *Paterson*, 1981]. Based on this same half width, an assumed basal yield stress of 100 kPa, and an ice density of 920 kg m^{-3}, equation (8) predicts a central height of 3160 m. Such close agreement clearly demonstrates the utility of Orowan's simple approach. However, the model does possess a minor flaw. Because equation (8) has the form of a parabola, it fails to predict a zero slope at an ice sheet's center ($x = 0$). Fortunately, the resulting discrepancy between theory and observation is generally small. Thus Orowan's model has gained recognition as a quick and accurate means of calculating equilibrium profiles.

In Figure 12, Orowan's model is applied to Mars, where the profiles of both polar caps have been calculated for three values of basal yield stress and two values of polar ice density. Basal yield stresses of 50–150 kPa characterize virtually all terrestrial ice sheets and glaciers and generally reflect basal temperatures that are within a few degrees of the melting point [*Nye*, 1959; *Weertman*, 1961*a*; *Paterson*, 1981]. As one might intuitively expect, the higher the yield stress, the greater the thickness of polar ice that can accumulate before the basal ice begins to deform. In a similar fashion, polar cap profiles are also affected by ice density; that is, it takes a taller column of low-density material to produce the same basal sheer stress generated by a short column of high-density material. This point is illustrated by comparing the profiles resulting from ice that is essentially dust-free (Figures 12*a* and 12*c*) with those produced by ice having a volumetric dust content of 40% (Figures 12*b* and 12*d*).

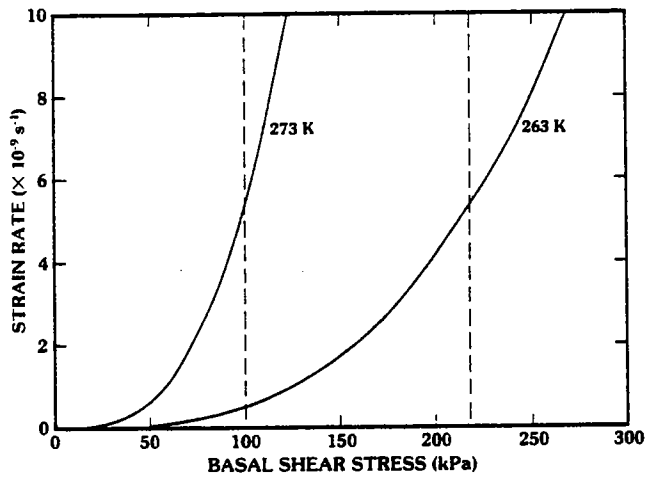

Fig. 10. The stress-strain relationship of ice at 273 K and 263 K. The deformation of ice at 273 K is often approximated by a perfectly plastic yield stress of 100 kPa; this yield stress corresponds to a strain rate of 5.3×10^{-9} s^{-1}. At 263 K the stress required to produce this same strain rate is 217 kPa.

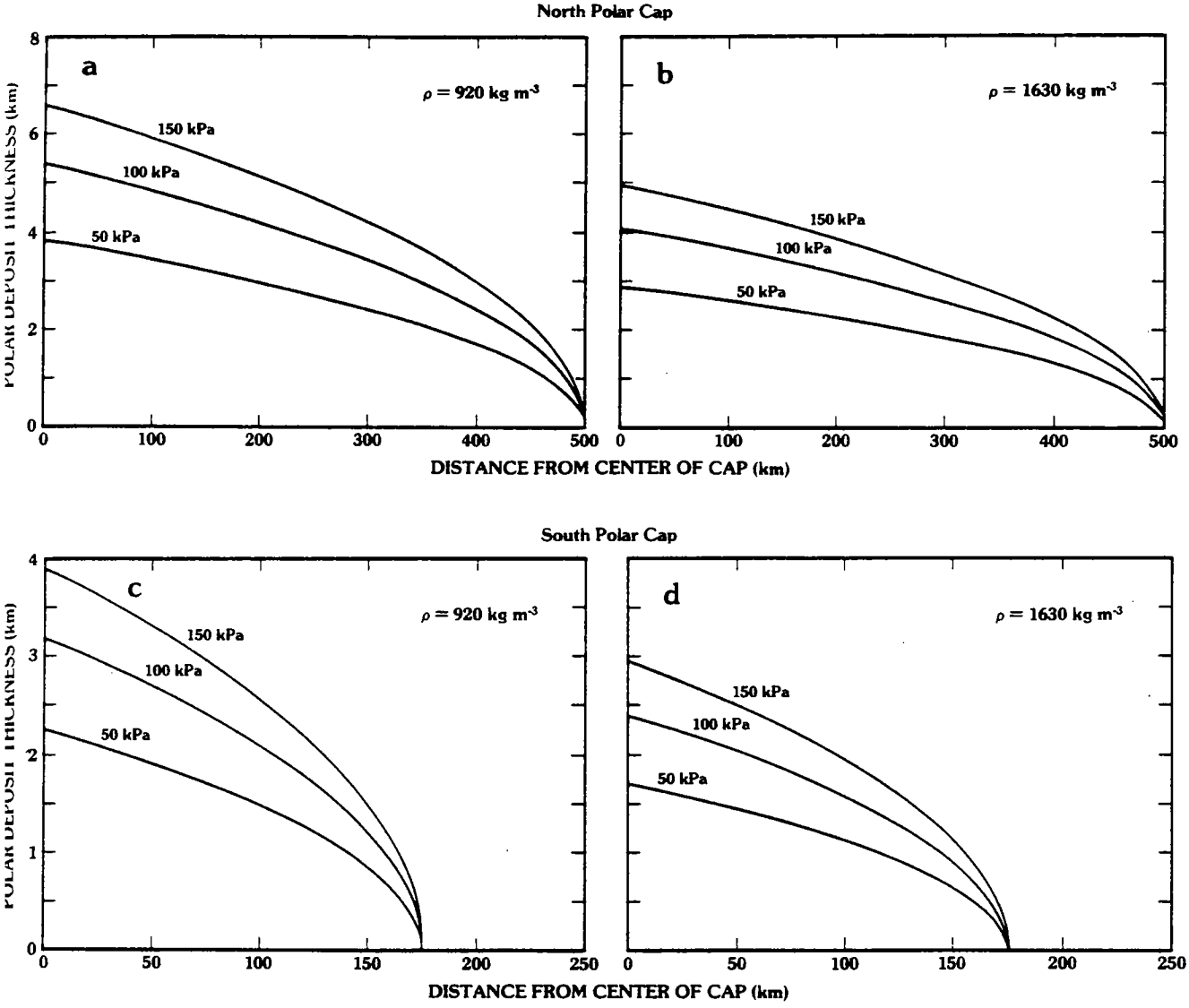

Fig. 12. Orowan profiles of the north and south polar caps calculated on the basis of three values of basal shear stress and two values of ice density. Since the basal topography is unkown, the profiles assume an unyielding horizontal bed. Should knowledge of the basal topography eventually be acquired, the theoretical polar profiles can be readily recalculated using an iterative form of Orowan's model developed by *Nye* [1952].

The equilibrium profiles of the northern cap (Figures 12*a* nd 12*b*) yield central heights (Table 3) that are consistent with he cap's inferred 4–6 km thickness [*Dzurisin and Blasius*, 1975]; owever, the corresponding profiles of the southern cap verpredict its apparent 1–2 km height by as much as a factor f 2. From these results, several general observations can be nade. Since neither polar cap has a central height that ubstantially exceeds those listed in Table 3, basal shear stresses n excess of 150 kPa appear unlikely, unless the volume fraction f dust entrained in the ice is substantially higher than currently elieved. Indeed, the close agreement between the inferred hickness of the northern cap and the equilibrium thicknesses alculated from the known range of terrestrial basal shear stresses 50–150 kPa) seems to argue for a basal temperature at or near he melting point. This conclusion is supported by the results f the thermal calculations presented in Figure 6 and Table , which show that the occurrence of basal melting at depths f 4–6 km is reasonable, given realistic values of thermal onductivity, geothermal heat flow, and salt-induced freezing oint depression.

There is, however, an alternative possibility that cannot be ruled out. It is that the polar caps are currently cold-based and have simply not yet achieved the required height necessary for their basal ice to undergo significant plastic deformation. This possibility appears particularly likely in the south, where the cap's inferred thickness of 1–2 km is approximately 40–70% smaller than the central heights predicted by the equilibrium

TABLE 3. Predicted Polar Cap Central Heights

Basal Yield Stress,	North Polar Cap		South Polar Cap	
kPa	920 kg m^{-3}	1630 kg m^{-3}	920 kg m^{-3}	1630 kg m^{-3}
50	3.82	2.87	2.26	1.70
100	5.40	4.06	3.19	2.40
150	6.61	4.97	3.91	2.94

Heights are in kilometers.

Polar cap central heights calculated using the profile model of *Orowan* [1949]. The half width L of the north polar cap is 5×10^5 m, while the half width for the south cap is $\sim 1.75 \times 10^5$ m. The actual heights inferred from Mariner 9 radio occultation data are 4–6 km for the north cap and 1–2 km for the south [*Dzurisin and Blasius*, 1975].

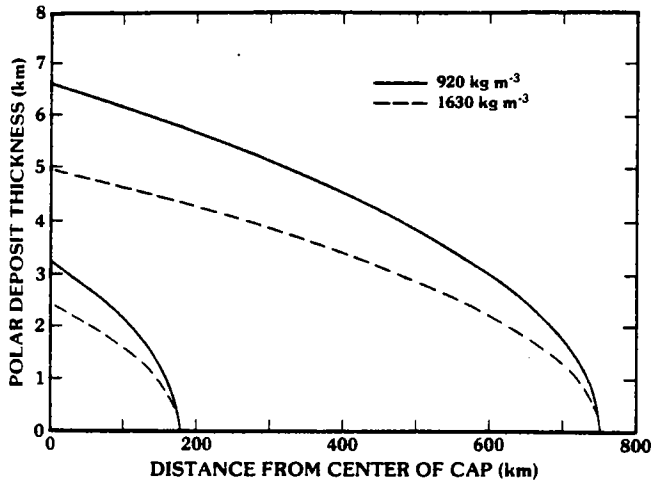

Fig. 13. South polar cap equilibrium profiles based on the half width of the perennial cap (175 km) and layered deposits (750 km). The perennial ice cap and layered deposits are often interpreted as related but otherwise distinct depositional units. Yet, this appearance could also result from an initially homogeneous unit whose surface has evolved under spatially varied conditions of insolation. For example, where the annually averaged incidence angle of incoming solar radiation has been large, the surface has retained its icy matrix, while at less favorable locations, the near surface has essentially been devolatilized. If this interpretation is correct, then it is the half width of the layered deposits that should determine the equilibrium profile of the cap. This results in a central height that is far greater than that predicted on the basis of the smaller perennial cap, thus aggravating the already sizable discrepancy with the profile height of 1–2 km inferred from Mariner 9 radio occultation data [*Dzurisin and Blasius*, 1975]. Note that the physical distinction between the perennial ice cap and layered deposits is less of a concern in the northern hemisphere, where the units are essentially coextensive.

profiles in Figures 12*c* and 12*d*. An even greater discrepancy results if one argues that the appropriate half width for the southern cap is not the 175-km radius of the perennial ice cover but is instead the 750-km radius of the layered deposits (Figure 13). In either case, the central height of the resulting equilibrium profile is clearly incompatible with the present best estimate of polar cap thickness [*Dzurisin and Blasius*, 1975]. This fact, combined with the results of the thermal calculations discussed earlier, strongly suggests that the south polar cap is currently frozen to its bed.

The foregoing analysis assumes that the mechanical properties of the polar deposits are essentially those of pure H_2O ice and that the flow of this ice can reasonably be approximated by a perfectly plastic yield stress of 100 kPa. In light of the evidence for dust and the possible presence of salts, however, there are valid reasons to question these assumptions. Compression tests conducted in the laboratory, and field observations of the shear zones in terrestrial glaciers, have shown that small quantities of entrained particulates (of the order of a few percent by volume) can sometimes increase, and other times decrease, the shear resistance of ice. However, once the volume fraction of entrained material exceeds ~5%, any further addition produces a consistent increase in ice hardness [*Swinzow*, 1962; *Goughnour and Andersland*, 1968; *Hooke et al.*, 1972]. On Mars the strengthening effect of entrained dust may be at least partially offset by the presence of other potentially weakening impurities such as salts, gas bubbles, and CO_2-H_2O clathrate [*Weeks and Asur*, 1967; *Miller and Smythe*, 1970]. The net synergistic effect of these contaminants on the mechanical properties of the Martian polar ice is presently unclear; however, laboratory compression tests of a range of compositional analogs could do much to reduce this uncertainty.

Finally, to complete this discussion of polar glacial flow on Mars, the more sophisticated profile models of *Nye* [1959] and *Weertman* [1961*b*] are briefly considered. In these models, equilibrium profiles are calculated, not on the assumption of perfect plasticity but on the basis of a more realistic flow law, similar to that given by equation (5). After *Nye* [1959], the resulting expression for the equilibrium profile of an ice sheet is

$$h^{2+1/m} = \left(\frac{2m+1}{m+1}\right)\left(\frac{1}{\rho_i g}\right)\left(\frac{a}{B}\right)^{1/m}\left(L^{1+1/m} - x^{1+1/m}\right) \quad (9)$$

where $m = (n+1)/2$, a is the accumulation rate (assumed to be constant over the surface of the cap), and B (equivalent to A^{-m} in *Nye*'s [1959] notation) is the constant in Weertman's velocity equation

$$u = B\tau_b^m \quad (10)$$

where the ice velocity u results from a combination of basal sliding and shear [*Weertman*, 1961*b*]. The value of B is a function of both the mechanical properties of the basal ice and the roughness of the bed [*Nye*, 1959; *Weertman*, 1961*b*]. Since these parameters are difficult, if not impossible, to assess directly, *Weertman* [1961*b*] has derived an alternative method for calculating B based on parameters that are more readily estimated or otherwise determined. For the case of an ice sheet resting on an unyielding horizontal surface, this expression is

$$B = a\left(\frac{2m+1}{m+1}\right)^m\left(\frac{1}{\rho_i g}\right)^m\left(\frac{L^{m+1}}{H^{2m+1}}\right) \quad (11)$$

where H is the observed central thickness of the cap [*Weertman*, 1961*b*]. Finally, noting that $m = 2$ when $n = 3$ and $h = H$ at $x = 0$, a little manipulation reduces equation (9) to

$$\left(\frac{h}{H}\right)^{2.5} + \left(\frac{x}{L}\right)^{1.5} = 1 \quad (12)$$

Inspection of equations (11) and (12) reveals that unlike Orowan's model, the equilibrium profile model of *Nye* [1959] and the related model of *Weertman* [1961*b*] require prior knowledge of an ice sheet's central height (or, equivalently, some independent means of determining a and B), a fact that limits, but does not preclude, the utility of these models as investigative tools. For example, one can use Orowan's model to predict a polar cap's central height and then apply the model of Nye to determine the cap's equilibrium profile. This two-step procedure has been applied to both polar caps in Figure 14, where the central heights were found by evaluating equation (8) at $x = 0$, assuming an ice density of 920 kg m^{-3} and a basal yield stress of 100 kPa. Inspection of the resulting profiles reveals that the principal shortcoming of Orowan's model, its failure to predict a zero slope at the center of an ice cap, is eliminated by the more realistic flow law inherent in the model of Nye (cf. Figures 12*a* and 12*c*).

It is important to emphasize that the equilibrium profiles illustrated in Figure 14, and elsewhere in this paper, are predicated on the assumption that the mass a polar cap gains by deposition over its surface is balanced by what it loses through

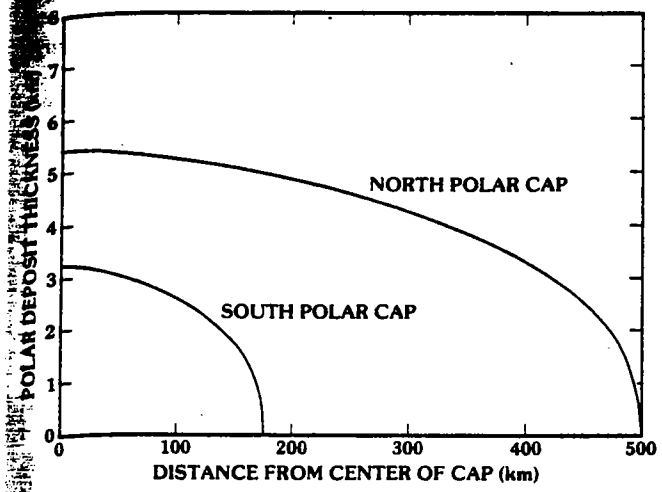

Fig. 14. Profiles of the north and south polar caps based on the more realistic equilibrium model of *Nye* [1959]. Note that the model correctly predicts a zero slope at the profile's center. As before, the profiles assume an unyielding horizontal base. Extensions of Nye's model, which take into account the effects of isostacy, basal topography, and the presence of a basal water layer, are discussed in detail by *Nye* [1959] and *Weertman* [1961*b*, 1966].

flow and ablation at its perimeter. Therefore, given such a condition, and a reasonable estimate of the accumulation rate, the amount of radial flow required to maintain the polar caps at their present size can be readily determined. On the basis of Viking data, *Pollack et al.* [1979] have estimated that the current rate of polar deposition is $\sim 10^{-4}$ m yr^{-1}, a figure consistent with the long-term rate deduced by *Cutts et al.* [1976] to account for the lack of craters visible in high-resolution images of the polar terrains. If we accept this estimate, and further assume a 100-kPa basal yield stress, equations (10) and (11) indicate that a radial flow velocity of $\sim 10^{-2}$ m yr^{-1} is required for the north polar cap to maintain an equilibrium state.

Evidence of such a small flow rate may be difficult to identify from Viking orbital imagery. For instance, ablation and concurrent erosion by strong seasonal winds may inhibit the formation of a discernable moraine at the edge of the cap. It is interesting to note, however, that at several locations in the north, a series of distinct ridges that parallel the cap's outer edge have been identified [*Howard et al.*, 1982]. While no unique mode of origin is indicated, *Howard et al.* [1982] have suggested glacial moraines as one possibility.

Although both radio occultation data and predictions based on established glacial theory appear to agree on the central height of the north polar cap, this observation alone is not proof that the cap has actually achieved an equilibrium profile. Yet our present knowledge of Martian polar topography is so poor that the cap's center is the only location where a reasonable height comparison can be made. This situation should improve dramatically in the early 1990s, when the United States hopes to place a radar altimeter into Mars polar orbit. The instrument, which will be flown aboard the Mars Observer spacecraft, is expected to yield high-resolution topographic data of virtually the entire planet.

In summary, the calculations presented in this section suggest that both basal melting and glacial flow are currently active processes in the polar regions of Mars. This is especially true in the north, where the 4–6 km thickness of the polar ice appears sufficient to insure conditions of high temperature and shear stress at the cap's true base. In the south, the thinness of the polar deposits makes glacial flow much less likely, although basal melting at some depth (i.e., Figure 4*b*) appears to be an inevitable consequence of the long-term existence of a net depositional environment at the poles [*Fanale et al.*, 1982].

DISCUSSION

The process of basal melting may be a key factor in understanding the evolution of the polar terrains and the climatic cycling of water on Mars. Several examples that illustrate the potential importance of this process are presented in the following discussion.

Origin of the Major Polar Reentrants

In a review of the various insolation-dependent models that have been proposed to explain the origin of the Martian polar terrains, *Blasius et al.* [1982] have remarked on the inability of these models to account for the broad linear depressions, like Chasma Boreale (85°N, 0°W) and Chasma Australe (87°S, 0°W), that are radially oriented and crosscut the outward spiraling polar troughs. One possibility suggested by *Clifford* [1980*a*,*b*] is that these features were formed by a jökulhlaup, the catastrophic discharge of a large subglacial reservoir of basal meltwater.

Weertman [1966, 1972] has shown that in regions where a terrestrial ice sheet is underlain by low-permeability bedrock, any water produced as a result of basal melting will flow in a thin layer from the central part of the ice sheet to its periphery. This flow is driven by the differential in hydrostatic head resulting from the radial decrease in overburden pressure exerted by the cap.

On Mars the polar caps may rest on a bed that is sufficiently permeable that any meltwater simply drains into a subpolar aquifer [*Clifford and Huguenin*, 1980; *Clifford*, 1980*a*]. Alternatively, in some regions the permeability of the bed may be low enough for the baseflow to be driven to the cap's frozen edge, where the accumulation of meltwater might eventually affect the local stability of the cap. For example, the buildup of subglacial hydrostatic pressure could result in the sudden flotation of ice at the cap's edge, thus triggering a catastrophic release of the accumulated reservoir of basal meltwater. Such a scenario may account for the preferential occurrence of most reentrants along the periphery of the polar deposits, as seen in the north at 84°N, 127°W and 84°N, 242°W or in the south at 83°S, 195°W and 84°S, 210°W.

While the model described above may provide a viable explanation for the origin of the smaller reentrants found near the edge of the polar deposits, it is less successful at explaining the larger features, such as Chasma Boreale and Chasma Australe, that originate much closer to the centers of their respective caps. One explanation for the origin for these features is suggested by the results of recent radio-echo soundings of the interior of the earth's Antarctic ice sheet. These soundings have revealed the presence of numerous basal lakes beneath the 3–4 km thickness of polar ice [*Oswald and Robin*, 1973; *Robin et al.*, 1977]. The lakes, which are believed to have formed as a result of geothermal melting, appear to be a minimum of several meters deep and cover individual areas as large as 180 km × 45 km [*Robin et al.*, 1977].

The discovery of basal lakes came as a surprise. While previous studies had suggested that large areas at the base of the Antarctic ice sheet had reached the melting point, calculations by *Weertman* [1966, 1972] suggested that any meltwater so derived

would flow toward the cap's edge as a thin (millimeters thick) sheet. However, *Oswald and Robin* [1973] showed that within the interior of the ice sheet, where surface slopes are small, the gradient in hydrostatic head imposed by the cap should be low enough for depressions within the bed to accumulate substantial (≥1 m) thicknesses of basal meltwater. They determined that the requirement for such accumulation is that the wall slope of the confining basin be at least 10 times greater than the local surface slope of the overlying ice sheet.

With regard to Mars, it seems likely that the bed which underlies the polar deposits experienced some degree of cratering prior to the initiation of significant polar deposition. Therefore near the center of the cap, where the likelihood is greatest that the basal ice has at one time reached the melting point, there may exist numerous areas that satisfy the minimum basin wall slope criterion outlined by *Oswald and Robin* [1973]. Should the rate of basal melting in these terrains exceed the maximum infiltration rate permitted by the underlying bed, a growing reservoir of meltwater might well accumulate within the confines of an ancient crater or impact basin. The continuation of this process would eventually lead to the breaching, and possible catastrophic drainage, of the subglacial lake.

The sudden release of meltwater from a basal lake could induce additional melting via the heat generated by turbulence and viscous dissipation within the flow and by friction between the moving water and overlying ice [*Shreve,* 1972; *Rothlisberger,* 1972; *Weertman,* 1972]. The resultant increase in baseflow could rapidly enlarge the original subglacial passage as water is forced down the hydrostatic pressure gradient toward the edge of the cap. In this way, a subglacial flood could grow to the point of breakout at the surface, resulting in the formation of such features as Chasma Boreale and Chasma Australe [*Clifford,* 1980*a,b*].

A potential problem with this scenario is that, once breached, would the wall of confining crater or basin erode rapidly enough to result in the catastrophic drainage of an interior lake? The answer to this question is by no means clear, particularly if the basal temperature is everywhere at the melting point; however, if the ice surrounding the basal lake is frozen to its bed, the problem is greatly simplified. With a frozen perimeter the upper surface of a basal lake could grow to an elevation in excess of the surrounding basal topography. Should the volume of the lake finally become large enough to destabilize the cap, catastrophic drainage would then be assured. Such a scenario is similar to the model proposed by *Nye* [1976] to explain the recurrent catastrophic drainage of Grimsvötn, a subglacial lake in the center of the Vatnajökull ice cap in Iceland.

Of course, variations on the basal melting hypothesis are possible. As in the case of Grimsvötn, a subglacial lake on Mars may occur, not in response to the regional geothermal heat flow but due to the presence of isolated "hot spots" or subglacial volcanic eruptions. While the occurrence of such thermal anomalies on Mars seems entirely reasonable, reliance on this same (essentially ad hoc) explanation for the origin of both Chasma Boreale in the north and Chasma Australe in the south may stretch credibility to the breaking point.

Partial support for a fluvial origin for the major polar reentrants comes from their resemblance to features, found elsewhere on the planet, whose origins are popularly attributed to the catastrophic release of groundwater. Of particular interest are the geomorphic similarities between Chasma Boreale (Figure 15*a*) and Ravi Vallis (1°S, 43°W) (Figure 15*b*). The differences between these two features can reasonably be attributed to their differing geologic environments. Consider, for example, the large blocks of disrupted crustal material visible on the floor of Ravi Vallis but absent in Chasma Boreale. The stability of the polar deposits is, to a large degree, due to both the high albedo of their ice-covered surface and the large incidence angle of incoming polar sunlight [*Howard,* 1978; *Blasius et al.,* 1982]. The disruption of the deposits by the catastrophic release of a subglacial lake would seriously alter this sensitive insolation balance. As a consequence of the large-scale exposure of low albedo dust and the creation of less favorable sun angles, the ice matrix would eventually sublime from the blocks of polar debris. The removal of this binding agent might then allow strong polar winds, confined by the channel, to erode and transport the resulting sediment down the length of the channel floor [*Cutts,* 1973*b*].

It should be noted that a fluvial origin of Chasma Boreale was first advocated by *Wallace and Sagan* [1979], who suggested that the direct absorption of sunlight within the polar ice could lead to significant near-surface melting, creating extensive polar lakes beneath a thin (~7 m) cover of ice. Early shaded relief maps of the north polar region, based on poor and incomplete Mariner 9 imagery, indicated the presence of a large crater (labeled "Zw") at the head of Chasma Boreale. *Wallace and Sagan* [1979] suggested that this association was probably not coincidental and that the impact that created Zw may have ruptured a near-surface lake whose outflow then carved the reentrant. However, subsequent Viking coverage of this region revealed that the crater Zw was actually an artifact created by viewing the head of Chasma Boreale at large incidence angles and under poor seeing conditions.

There are also reasons to question the likelihood of near-surface polar lakes. *Wallace and Sagan* [1979] based their calculations on the assumption that there would be little attenuation of sunlight through the top 7 m of ice. Yet the evidence for the presence of a significant entrained dust component would seem to contradict this assumption [e.g., *Kieffer et al.,* 1976]. Indeed, even if one assumes a bulk extinction coefficient as low as 1 m^{-1}, a value typical of relatively clean glacial ice on earth [*Grenfell and Maykut,* 1977], less than 5% of the incoming solar radiation would penetrate below a depth of 3 m. Thus, given a reasonable value for the thermal conductivity of the intervening ice, the resulting heat balance makes the existence of any near-surface reservoir of liquid water extremely unlikely.

Clearly a fluvial origin is not the only possible explanation for Chasma Boreale and the other polar reentrants, but it appears to be a viable candidate if basal melting has in fact occurred.

Storage of an Ancient Martian Ice Sheet

In the Martian northern plains and near the south polar cap, Viking Orbiter imagery has revealed a number of features that bear a strong resemblance to Iceland's table mountains [*Allen,* 1979; *Hodges and Moore,* 1979]. Because table mountains on earth are formed by subglacial volcanic eruptions, the discovery of possible analogs on Mars has led to speculation that extensive ice sheets may once have covered sizable areas of both the northern and southern hemispheres. From an examination of the height of these landforms, *Allen* [1979] has determined that the original ice thickness may have ranged from 100 to 1200 m. Such estimates have prompted *Arvidson et al.* [1980] to

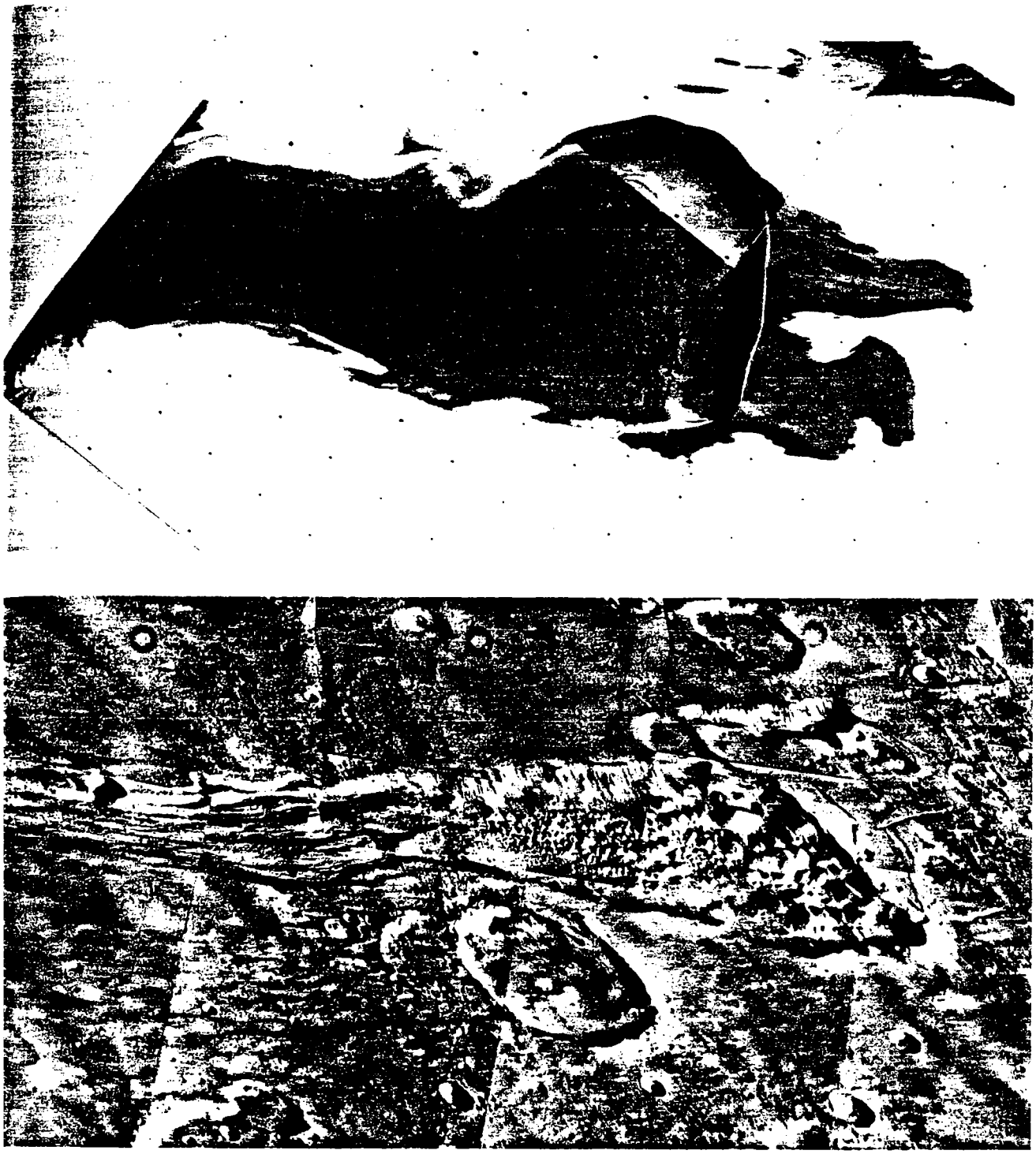

Fig. 15. Viking Orbiter photographs of (*a*) Chasma Boreale (85°N, 0°W) and (*b*) Ravi Vallis (1°S, 43°W). The scale of the Chasma Boreale mosiac (057B43, 057B44, 057B45) is approximately 135 km × 70 km, while the mosiac of Ravi Vallis (P-16983) shows a 150-km portion of its length.

gue that the problems associated with the removal and storage such a large volume of ice make a subglacial origin for the ble mountains difficult to support.

While legitimate questions may exist regarding the true origin the Martian "table mountains," the objections raised by vidson *et al.* [1980] are not by themselves fatal. Consider st the problem of storage. Repeated impacts have clearly ayed an important role in the structural development of the artian crust [*Fanale,* 1976; *Carr,* 1979]. On the moon, which has experienced a similar cratering history, studies of the crust's near-surface seismic propagation characteristics suggest that it is brecciated to a depth of roughly 20 km [*Carr,* 1979]. Gravitationally scaling these lunar results to Mars indicates that the Martian crust may retain significant porosity down to a depth of approximately 10 km and that its total pore volume may be sufficient to store a quantity of water equal to a 1.5-km layer averaged over the planet's surface [*Clifford,* 1981*a*; 1984*a*]. If these calculations are correct, then the Martian crust

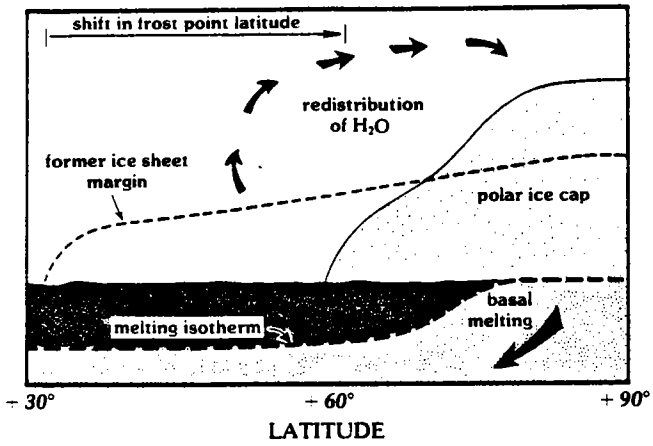

Fig. 16. A possible mechanism for the removal and subsurface storage of an ancient ice sheet. If, following a period of extensive glaciation, temperatures increased at equatorial and temperate latitudes, the subsequent retreat of the frost point latitude would have caused the periphery of the ice sheet to ablate and redistribute itself poleward. Through the process of basal melting, the ice sheet might then have been stored as groundwater [*Clifford*, 1980*c*, 1984*a*].

could easily accommodate the volume of H_2O contained in a sizable ancient ice sheet. The major problem that remains, therefore, is the identification of a process by which this potential storage capacity could have been filled.

Ice will persist on the Martian surface only at those latitudes where the temperature remains continuously below the frost point. If Mars once possessed extensive polar ice sheets, then this fact may help to account for their subsequent disappearance. Consider, for example, a situation in which the climate warmed after the ice sheets had reached their maximum areal extent. With the rise of mean annual temperatures at equatorial and temperate latitudes, the position of the frost point latitude would have migrated toward the poles. As this latitude passed the outer perimeter of the ice sheet, the ice would have begun to ablate and redistribute itself poleward via cold trapping. As a consequence, what the ice sheet lost in areal extent it gained in thickness at the poles. With this added thickness the melting isotherm would have risen to maintain its equilibrium depth from the surface, resulting in the onset of basal melting (Figure 16).

If the area involved in basal melting were equal to the present extent of the north and south polar deposits and if the value of the geothermal heat flux was $\sim 3 \times 10^{-2}$ W m^{-2}, then a 500-m-thick ice sheet that once covered 40% of the planet's surface could have been introduced into the crust as groundwater in as little as a few million years.

Mass Balance of the Polar Terrains

It is generally accepted that the polar layered deposits owe their origin and apparent youthfulness to the annual deposition of dust and H_2O and that the magnitude of this deposition has been modulated by periodic variations in insolation due to changes in the Martian orbital elements and obliquity [*Cutts* et al., 1979; *Pollack et al.*, 1979; *Toon et al.*, 1980]. On the basis of their evident thickness and the absence of any craters with diameters larger than 300 m, it is estimated that the present deposits accumulated on a time scale of $\lesssim 10^8$ years [*Cutts et al.*, 1976; *Pollack et al.*, 1979]. However, there appears to be a serious problem inherent in this depositional model [*Clifford and Huguenin*, 1980]. Recent studies suggest that the climatic conditions conducive to polar deposition are not unique to the present epoch but have existed throughout most of Martian geologic history [*Fanale et al.*, 1982, 1986]. Given such conditions and the apparent youthfulness of the present polar deposits, how does one account for the lack of any older material at the poles?

One possible answer is that periods of intense polar erosion have alternated with climatic periods of accumulation [*Carr*, 1981]. Such erosion must be extremely efficient in redistributing the resulting debris if it is to eliminate any previous record of polar construction. However, no significant variable in the Martian climate with a period greater than the $\sim 10^6$-year variation in orbital eccentricity has yet been identified [*Ward*, 1974, 1979]. Further, the periodic changes in insolation that result from the interaction of the these time-varying astronomical parameters appear to fall well short of that required to counter the net long-term deposition of ice and dust at the poles [*Fanale et al.*, 1982, 1986]. This conclusion is supported by both the inferred 10^7–10^8 year age of the present deposits and by the lack of observational evidence indicative of any widespread erosion of the polar laminae [*Howard et al.*, 1982].

Another possible solution to the mass balance problem has been proposed by *Toon et al.* [1980], who suggest that new polar laminae are simply created at the expense of the old. This possibility is raised by current models of the evolution of the polar troughs [*Howard*, 1978; *Howard et al.*, 1982]. These features, which form the conspicuous spiral patterns visible in the remnant polar caps (Figure 2), are thought to originate near the edge of the deposits and migrate toward the pole. This migration is thought to be driven by the preferential sublimation of ice from the equatorward facing slopes of the troughs. Dust, liberated from the polar ice, may then be scavenged by polar winds and redistributed over the planet, while the sublimed ice may simply be recycled by cold trapping on the poleward facing slopes and on the flats that separate the polar troughs. By these processes, *Toon et al.* [1980] suggest that the polar deposits have essentially reached a state of equilibrium whereby ancient ($\gtrsim 10^9$ year old) polar material is continually reworked, maintaining a comparatively youthful surficial appearance in spite of its great age.

However, based on a detailed study of polar stratigraphy made from high-resolution Viking Orbiter imagery, *Howard et al.* [1982] have argued that a simple local recycling of the polar laminae is untenable. They support this conclusion by citing observational evidence that the erosion of equatorward facing scarps has not kept pace with layer deposition near the poles, requiring a net long-term accumulation of material within the polar terrains [*Howard et al.*, 1982].

To summarize, it appears that any solution to the mass balance problem must (1) be consistent with theoretical models of the Martian climate, which indicate that a net depositional environment has existed at the poles throughout most of the planet's geologic history [*Fanale et al.*, 1982, 1986], (2) be able to account for the observational evidence that the evolution of the polar terrains has indeed been dominated by depositional processes [*Howard et al.*, 1982], (3) be able to accommodate a rate of deposition, implied by the lack of craters within the deposits, of at least 10^{-4} m yr^{-1} [*Cutts et al.*, 1976; *Pollack et al.*, 1979], and (4) satisfy all of the previous conditions within the constraint imposed by the apparent deficit of material that currently exists at the poles.

There are two explanations that appear to satisfy these requirements. The first is based on the evidence for polar

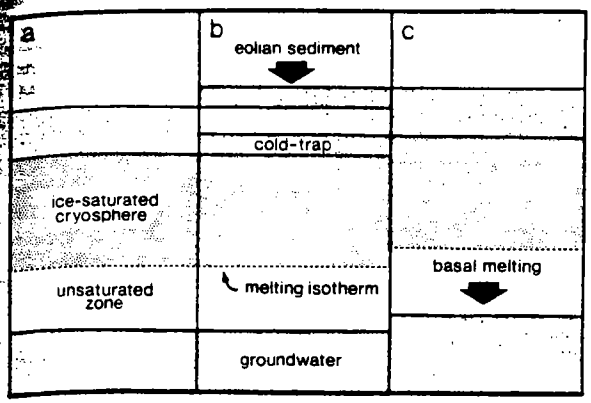

Fig. 17. Basal melting at temperate latitudes as the result of eolian deposition.

wandering, summarized by *Schultz* [1985]. Within the equatorial region of Mars, several extensive antipodal layered deposits have been identified that bear certain striking similarities to the present polar layered terrains [*Schultz and Lutz-Garihan,* 1981*a,b*]. To account for these features, *Schultz* [1985] has proposed that over a time scale of several billion years, the crust of Mars has undergone a major reorientation in relation to its spin axis. He attributes this movement to changes in the planet's moment of inertia caused by the formation of the Tharsis volcanic province. While the actual dynamics necessary to produce this shift are presently unclear, the slow migration of the geographic location of the poles does provide a possible solution to the mass balance problem, given that this migration has spanned geologic time (distributing the debris over a wide area) and that the age of the present polar locations is $\lesssim 10^8$ years (consistent with the accumulated volume of the deposits).

However, if significant polar wandering has not occurred, or if it was restricted to a period very early in Martian geologic history, then an alternative solution to the mass balance problem must be found. The process of basal melting may provide this solution [*Clifford and Huguenin,* 1980]. Once the polar deposits have reached the required thickness for basal melting, they will have achieved a condition of relative equilibrium, where the accumulation of H_2O at the ice cap's surface will eventually be offset by melting at its base. Indeed, as noted earlier, a geothermal heat flux of 3×10^{-2} W m^{-2} K^{-1} could easily keep pace with an H_2O deposition rate as high as 5×10^{-3} m yr^{-1}. Therefore the occurrence of basal melting is consistent with both the results of climatic models [*Fanale et al.,* 1982, 1986] and the observational evidence [*Howard et al.,* 1982], indicating that a long-term net depositional environment has existed at the poles.

Of course, while basal melting may resolve the eventual fate of the polar ice, there still remains the problem of the polar dust. Fortunately, the dust mass balance is significantly more tractable, in that the nonvolatile nature of the dust allows it to be physically removed from the polar troughs by surficial processes of erosion and redistributed to nonpolar latitudes. Alternatively, the possibility of glacial flow suggests that any basal debris may eventually be transported to the periphery of the cap, where it may be scoured away by strong seasonal winds.

Basal Melting at Temperate Latitudes

The discussion of basal melting presented so far has been limited to the polar regions; however, it is important to note that the occurrence of basal melting is not necessarily restricted to the region occupied by the visible polar caps. Indeed, wherever ice is present at the base of the cryosphere, the deposition and long-term retention of material at the surface will eventually lead to basal melting.

For example, based on an analysis of Mariner 9 imagery, *Soderblom et al.* [1973*b*] have presented evidence that suggests that the terrains poleward of 35° may be mantled by eolian debris. While this interpretation has recently been questioned [*Kahn et al.,* 1986], the existence of such a mantle is consistent with both theoretical arguments [*Pollack et al.,* 1979] and Viking Lander 2 images [*Wall,* 1981], which indicate that dust raised during the major perihelion dust storms is preferentially deposited at mid- to high latitudes during the formation of the seasonal polar caps. The physical evolution of such eolian mantles has significant implications for both the long-term exchange of H_2O between the atmosphere and regolith and the possibility of basal melting at nonpolar latitudes.

The interface between the occurrence of perennial ground ice and ice-free regolith on Mars is determined by the depth to which the annual thermal wave elevates regolith temperatures above the frost point (Figure 17*a*). Clearly, the deposition of a layer of dust on the surface will result in a corresponding upward displacement of this interface within the regolith (Figure 17*b*). The coldtrap, so formed, will act as a net sink for atmospheric water vapor until either its pore volume is filled with ice or its pores become so obstructed that they no longer serve as adequate passages for the diffusion of H_2O. If the dust layer is stable against erosion or continues to accumulate, the added insulation will eventually lead to basal melting (Figure 17*c*).

A simple calculation can provide a rough estimate of the quantity of water that may be involved in this process on an annual basis. If we assume that a 10-μm-thick dust layer with a porosity of 50% is deposited annually at latitudes poleward of 40°N (consistent with the calculations of *Pollack et al.* [1979]), then as much as 0.13 km^3 of atmospheric H_2O could be retained as perennial ground ice each year. Clearly, if the physical and thermal properties of this surface layer are similar to those found at the base of the cryosphere, the eventual rise of the melting isotherm should release an equivalent amount of ground ice as meltwater. If deposition is occurring in the south as well, this annual figure will then be doubled.

Of course, the processes of cold trapping and basal melting can also operate in reverse. At those times and at those locations where the regolith undergoes preferential erosion (as the region surrounding Viking Lander 2 periodically must, in order to prevent the burial of its boulder strewn landscape) the annual thermal wave will penetrate deeper into the regolith; thus, where perennial ground ice once existed, the near-surface regolith will now be dry. At depth, the melting isotherm will eventually respond to the long-term erosion of surface material by retreating deeper into the crust. This displacement will again create a coldtrap but this time at the base of the cryosphere, where it will serve as a sink for any subpermafrost H_2O that may exist there [*Clifford,* 1980*d*, 1982*a*].

The preceding arguments suggest that the existence of long-term sources and sinks of atmospheric H_2O on Mars are closely linked to the erosional and depositional evolution of its surface [*Clifford,* 1982*b*; *Zent et al.,* 1986]. If so, then the annual and climatic behavior of atmospheric H_2O is likely to be more complex and dynamic than is indicated by present models of atmosphere-regolith exchange.

Some Further Considerations

The potential importance of basal melting on Mars is not restricted to the examples cited above. It has also been discussed with regard to the origin of the etched plains and braided ridges of the south polar region [*Howard*, 1981], as a key process in the Martian hydrologic cycle [*Clifford*, 1981*b*, 1984*a*], and in connection with the possible survival of ancient Martian lifeforms in polar basal lakes [*Clifford*, 1983].

Regardless of whether basal melting has in fact occurred on Mars, the polar terrains clearly hold important clues to the planet's climatic history. For this reason, they are likely to be high-priority objectives of any future exploration. While a variety of techniques are likely to be employed in such an investigation, two, active seismic exploration and radio echo sounding, appear particularly promising because of their ability to probe the physical properties, internal structure, and basal topography of the deposits over large areas and to great depths [*Robin et al.*, 1969, 1977; *Tittmann*, 1979; *Paterson*, 1981]. Of relevance to the present discussion is the fact that both methods have been successfully applied to the detection of basal melting on earth [*Dewart*, 1976; *Oswald and Robin*, 1973]. Thus the use of either technique in the exploration of the Martian polar terrains should have the added benefit of providing the first unambiguous test of basal melting on Mars.

CONCLUSION

If ice is present throughout the cryosphere anywhere on Mars, it is most likely at the poles. Given this condition, the deposition of dust and H_2O at the surface will ultimately result in a situation where the equilibrium depth to the melting isotherm has been exceeded, melting ice at the base of the cryosphere until thermal equilibrium is once again established. Should deposition persist, the deposits will ultimately reach a thickness where melting will occur at their actual base. In the north, thermal calculations and consideration of the cap's theoretical equilibrium profile suggest that the temperature at the base of the deposits is at or near the melting point, while in the south this same evidence suggests the cap is now frozen to its bed. Even if "true" basal melting does not presently occur, melting at the base of the cryosphere appears to be an inevitable consequence of polar deposition. The occurrence of such melting could have a profound affect on the evolution of the polar terrains and the long-term climatic cycling of H_2O. Investigations by the Mars Observer spacecraft and its likely successors should provide important tests of this hypothesis.

NOTATION

a polar accumulation rate, m yr^{-1}.
A flow law constant, s^{-1} Pa^{-3}.
A_b time-averaged polar cap albedo.
A_0 temperature invariant flow law constant, $\sim 4.3 \times 10^{-4}$ s^{-1} kPa^{-3}.
B constant in ice velocity equation, m yr^{-1} Pa^{-2}
C_m specific heat of polar deposits, J kg^{-1} K^{-1}.
e orbital eccentricity.
g mean Martian acceleration of gravity, 3.73 m s^{-2}
h height of ice sheet profile, m.
H central height of cap, m.
i obliquity, deg.
$\langle I \rangle_{pole}$ mean polar insolation, W m^{-2}.
k_{eff} effective thermal conductivity of polar deposits, W m^{-1} K^{-1}.
L half-width of polar cap, m.
m $= (n+1)/2$.
n exponent in flow law.
P period of temperature variation, s.
Q activation energy for creep, J mol^{-1}.
Q_f frictional heat due to glacial sliding, W m^{-2}.
Q_g geothermal heat flux, W m^{-2}.
R gas constant, 8.314 J mol^{-1} K^{-1}.
S_0 Martian solar constant, 600 W m^{-2}.
T temperature, K.
T_{mp} melting point temperature, K.
T_{ms} mean polar surface temperature, K.
T_s mean annual polar surface temperature, K.
u polar ice velocity, m s^{-1}.
V_b basal sliding velocity, m s^{-1}.
x distance from center of cap, m.
β skin depth, m.
ϵ emissivity.
$\dot{\epsilon}$ strain rate, s^{-1}.
ρ_i density of polar deposits, kg m^{-3}.
σ Stefan–Boltzman constant, 5.67×10^{-8} W m^{-2} K^{-4}.
τ shear stress, Pa.
τ_b basal shear stress, Pa.

Acknowledgments. I would like to thank John Hollin, Bob Huguenin, George McGill, Mark Cintala, Fraser Fanale, David Paige, Michael Carr, Peter Schultz, Bruce Bills, Jim Zimbelman, Stephanie Tindell, Bill Irvine, Peter Schloerb, Daniel Hillel, and Julie Clifford, all of whom reviewed earlier versions of this paper and provided many valuable suggestions for its improvement. Much of this research was supported under NASA grant NSG 7405. Additional support was provided by the Lunar and Planetary Institute (LPI), which is operated by the Universities Space Research Association under contract NASW-4066 with the National Aeronautics and Space Administration. This paper is LPI contribution 620.

REFERENCES

Anderson, D. M., and A. R. Tice, The unfrozen interfacial phase in frozen soil water systems, in *Ecological Studies: Analysis and Synthesis, vol. 4*, edited by A. Hadas, D. Swartzendruber, P. E. Rijtema, M. Fuchs, and B. Yaron, pp. 107–124, Springer-Verlag, New York, 1973.

Anderson, D. M., E. S. Gaffney, and P. F. Low, Frost phenomena on Mars, *Science, 155*, 314–322, 1967.

Allen, C. C., Volcano-ice interactions on Mars, *J. Geophys. Res., 84*, 8048–8059, 1979.

Arvidson, R. E., K. A. Goettel, and C. M. Hohenberg, A post-Viking view of Martian geologic evolution, *Rev. Geophys., 18*, 565–603, 1980.

Arvidson, R. E., E. A. Guinness, H. J. Moore, J. Tillman, and S. D. Wall, Three Mars years: Viking Lander 1 imaging observations, *Science, 222*, 463–468, 1983.

Banin, A., and D. M. Anderson, Effects of salt concentration changes during freezing on the unfrozen water content of porous materials, *Water Resour. Res., 10*, 124–128, 1974.

Barker, E. S., R. A. Shorn, A. Woszczyk, R. G. Tull, and S. J. Little, Mars: Detection of atmospheric water vapor during the southern hemisphere spring and summer season, *Science, 170*, 1308–1310, 1970.

Blasius, K. R., J. A. Cutts, and A. D. Howard, Topography and stratigraphy of Martian polar layered deposits, *Icarus, 50*, 140–160, 1982.

Brass, G. W., Stability of brines on Mars, *Icarus, 42*, 20–28, 1980.

Carr, M. H., Formation of Martian flood features by release of water from confined aquifers, *J. Geophys. Res., 84*, 2995–3007, 1979.

Carr, M. H., *The Surface of Mars*, 232 pp., Yale University Press, New Haven, Conn., 1981.

Carr, M. H., Mars: A water-rich planet, *Icarus, 68*, 187–216, 1986.

Mariner 1969 infrared radiometer results: Temperatures and thermal properties of the Martian surface, *Astron. J., 76,* 719–728, 1971.
Nye, J. F., The flow of glaciers and ice-sheets as a problem in plasticity, *Proc. R. Soc. London, Ser A, 207,* 554–572, 1951.
Nye, J. F., A method of calculating the thicknesses of the ice-sheets, *Nature, 169,* 529–530, 1952.
Nye, J. F., The motion of ice sheets and glaciers, *J. Glaciology 3,* 493–507, 1959.
Nye, J. F., Water flow in glaciers: Jökulhlaups, tunnels and veins, *J. Glaciol., 17,* 181–207, 1976.
Nye, J. F., and F. C. Frank, Hydrology of the intergranular veins in a temperate glacier,in *Symposium on the Hydrology of Glaciers,* pp. 157–161, International Assoc. Scientific Hydrol., Cambridge, England, 1973.
Nye, J. F., and S. Mae, The effect of non-hydrostatic stress on intergranular water veins and lenses in ice, *J. Glaciol., 11,* 81–101, 1972.
Orowan, E., Remarks at joint meeting of the British Glaciological Society, the British Rheologists Club and the Institute of Metals, *J. Glaciol., 1,* 231–236, 1949.
Oswald, G. K. A., and G. de Q. Robin, Lakes beneath the Antarctic ice sheet, *Nature, 245,* 251–254, 1973.
Paige, D. A., and A. P. Ingersoll, Annual heat balance of Martian polar caps: Viking observations, *Science, 228,* 1160–1168, 1985.
Paige, D. A., and H. H. Kieffer, Non-linear frost albedo feedback on Mars: Observations and models, in Workshop on the Evolution of the Martian Atmosphere, *LPI Tech Rpt. 86-07,* pp. 33–34, Lunar and Planet. Inst., Houston, Tex., 1986.
Pang, K., J. M. Ajello, C. W. Hord, and W. G. Egan, Complex refractive index of Martian dust: Mariner 9 ultraviolet observations, *Icarus, 27,* 55–67, 1976.
Paterson, W. S. B., The *Physics of Glaciers,* 2nd ed., 380 pp., Pergamon, New York, 1981.
Penner, E., Thermal conductivity of frozen soils, *Can. J. Earth Sci., 7,* 982–987, 1970.
Pollack, J. B., and D. C. Black, Implications of the gas compositional measurements of Pioneer Venus for the origin of planetary atmospheres, *Science, 205,* 56–59, 1979.
Pollack, J. B., D. Colburn, F. M. Flasar, R. Kahn, C. E. Carlston, and D. Pidek, Properties and effects of dust particles suspended in the Martian atmosphere, *J. Geophys. Res., 84,* 2929–2945, 1979.
Puri, B. R., and K. Murari, Studies in surface area measurements of soils, 1, Comparison of different methods, *Soil Sci., 96,* 331–336, 1963.
Raymond, C. F., and W. D. Harrison, Some observations on the behavior of the liquid and gas phases in temperate glacier ice, *J. Glaciol., 14,* 213–233, 1975.
Ricq-de Bouard, M., Migration of insoluble and soluble impurities in temperate ice: Study of a vertical ice profile through the Glacier du Mont de Lans (French Alps), *J. Glaciol., 18,* 231–238, 1977.
Robin, G. de Q., S. Evans, and J. T. Bailey, Interpretation of radio echo sounding in polar ice sheets, *Philos. Trans. R. Soc. London, Ser. A, 265,* 437–505, 1969.
Robin, G. de Q., D. J. Drewry, and D. T. Meldrum, International studies of ice sheet and bedrock, *Philos. Trans. R. Soc. London, Ser. B, 279,* 185–196, 1977.
Rossbacher, L. A., and S. Judson, Ground ice on Mars: Inventory, distribution, and resulting landforms, *Icarus, 45,* 39–59, 1981.
Rothlisberger, H., Water pressure in intra- and subglacial channels, *J. Glaciol., 11,* 177–203, 1972.
Sanger, F. J., Degree-days and heat conduction in soils, in *Proceedings of the International Conference on Permafrost,* pp. 253–262, National Academy of Sciences, Washington D. C., 1963.
Schultz, P. H., Polar wandering on Mars, *Sci. Am., 253,* 94–102, 1985.
Schultz, P. H., and A. B. Lutz-Garihan, Equatorial paleo-poles on Mars, *Lunar Planet. Sci. Conf., XII,* 946–948, 1981*a*.
Schultz, P. H. and A. B. Lutz-Garihan, Ancient polar locations on Mars: Evidence and implications, in *Papers presented to the Third International Colloquium on Mars,* pp. 229–231, Lunar and Planet. Inst., Houston, Tex., 1981*b*.
Sharp, R. P., Ice on Mars, *J. Glaciol., 13,* 173–185, 1974.
Shreve, R. L., Movement of water in glaciers, *J. Glaciol., 11,* 205–214, 1972.
Smoluchowski, R., Mars: Retention of ice, *Science, 159,* 1348–1350, 1968.
Soderblom, L. A., M. C. Malin, J. A. Cutts, and B. C. Murray, Mariner 9 observations of the surface of Mars in the north polar region, *J. Geophys. Res., 78,* 4197–4210, 1973*a*.
Soderblom, L. A., T. J. Kreidler, and H. Masursky, Latitudinal distribution of a debris mantle on the Martian surface, *J. Geophys. Res., 78,* 4117–4122, 1973*b*.
Squyres, S. W., The evolution of dust deposits in the Martian north polar region, *Icarus, 40,* 244–261, 1979.
Swinzow, G. K., Investigation of the shear zones in the ice sheet margin, Thule area, Greenland, *J. Glaciol., 4,* 215–229, 1962.
Tittmann, B. R., Brief note for consideration of active seismic exploration on Mars, *J. Geophys. Res., 84,* 7940–7942, 1979.
Toksöz, M. N., and A. T. Hsui, Thermal history and evolution of Mars, *Icarus, 34,* 537–547, 1978.
Toon, O. B., J. B. Pollack, W. Ward, J. A. Burns, and K. Bilski, The astronomical theory of climatic change on Mars, *Icarus, 44,* 552–607, 1980.
Toulmin, P., III, A. K. Baird, B. C. Clark, K. Keil, H. J. Rose, Jr., P. H. Evans, and W. C. Kelliher, Geochemical and mineralogical interpretation of the Viking inorganic chemical results, *J. Geophys. Res., 82,* 4625–4634, 1977.
Wall, S. D., Analysis of condensates formed at the Viking 2 lander site: The first winter, *Icarus, 47,* 173–183, 1981.
Wallace, D., and C. Sagan, Evaporation of ice in planetary atmospheres: Ice-covered rivers on Mars, *Icarus, 39,* 385–400, 1979.
Ward, W. R., Climatic variations on Mars, 1, Astronomical theory of insolation, *J. Geophys. Res., 79,* 3375–3386, 1974.
Ward, W. R., Present obliquity oscillations of Mars: Fourth-order accuracy in orbital e and I, *J. Geophys. Res., 84,* 237–241, 1979.
Weeks, W., and A. Asur, The mechanical properties of sea ice, *CRREL Rep. II-C3,* 94 pp., Cold Reg. Res. and Eng. Lab., Hanover, N.H., 1967.
Weertman, J., Mechanism for the formation of inner moraines found near the edge of cold ice caps and ice sheets, *J. Glaciol., 3,* 965–978, 1961*a*.
Weertman, J., Equilibrium profile of ice caps, *J. Glaciol., 3,* 953–964, 1961*b*.
Weertman, J., The theory of glacier sliding, *J. Glaciol., 5,* 287–303, 1964.
Weertman, J., Effect of a basal water layer on the dimensions of ice sheets, *J. Glaciol., 6,* 191–207, 1966.
Weertman, J., General theory of water flow at the base of a glacier or ice sheet, *Rev. Geophys., 10,* 287–333, 1972.
Weertman, J., Creep of ice, in *Physics and Chemistry of Ice,* edited by E. Whalley, S. J. Jones and L. W. Gold, pp. 320–337, Royal Society of Canada, Ottawa, Canada, 1973.
Zent, A. P., F. P. Fanale, J. R. Salvail, and S. E. Postawko, Distribution and state of H_2O in the high-latitude shallow subsurface of Mars, *Icarus, 67,* 19–36, 1986.

S. M. Clifford, Lunar and Planetary Institute, 3303 NASA Road 1, Houston, TX 77058.

(Received November 10, 1986;
accepted January 15, 1987.)